© 2023. Published by The Company of Biologists Ltd | Development (2023) 150, dev201189. doi:10.1242/dev.201189

RESEARCH ARTICLE

Canonical Wnt signaling regulates soft palate development by mediating ciliary homeostasis

Eva Janečková, Jifan Feng, Tingwei Guo, Xia Han, Aileen Ghobadi, Angelita Araujo-Villalba, Md Shaifur Rahman, Heliya Ziaei, Thach-Vu Ho, Siddhika Pareek, Jasmine Alvarez and Yang Chai*

ABSTRACT

Craniofacial morphogenesis requires complex interactions involving different tissues, signaling pathways, secreted factors and organelles. The details of these interactions remain elusive. In this study, we have analyzed the molecular mechanisms and homeostatic cellular activities governing soft palate development to improve regenerative strategies for individuals with cleft palate. We have identified canonical Wnt signaling as a key signaling pathway primarily active in cranial neural crest (CNC)-derived mesenchymal cells surrounding soft palatal myogenic cells. Using *Osr2-Cre;β-catenin*$^{fl/fl}$ mice, we show that Wnt signaling is indispensable for mesenchymal cell proliferation and subsequently for myogenesis through mediating ciliogenesis. Specifically, we have identified that Wnt signaling directly regulates expression of the ciliary gene *Ttll3*. Impaired ciliary disassembly leads to differentiation defects in mesenchymal cells and indirectly disrupts myogenesis through decreased expression of *Dlk1*, a mesenchymal cell-derived pro-myogenesis factor. Moreover, we show that siRNA-mediated reduction of *Ttll3* expression partly rescues mesenchymal cell proliferation and myogenesis in the palatal explant cultures from *Osr2-Cre;β-catenin*$^{fl/fl}$ embryos. This study highlights the role of Wnt signaling in palatogenesis through the control of ciliary homeostasis, which establishes a new mechanism for Wnt-regulated craniofacial morphogenesis.

KEY WORDS: Wnt signaling, Soft palate development, Palatogenesis, Ciliogenesis

INTRODUCTION

Organ morphogenesis is a complex process involving homeostatic cellular activities as well as reciprocal tissue-tissue interactions with signals relayed by secreted factors (Strand et al., 2010). The soft palate is an anatomical structure with unique functions, and its embryonic development involves interplay among cranial neural crest (CNC)-derived mesenchymal cells, mesoderm-derived myogenic cells and ectoderm-derived epithelial cells, making it an excellent model for unraveling the intricate morphogenetic tissue-tissue communications during craniofacial development (Grimaldi et al., 2015; Li et al., 2019; Sugii et al., 2017). Of particular interest is the role of CNC-derived mesenchymal cells and factors derived from them, which mediate communication with myogenic precursors during early craniofacial muscle development. The majority of these factors, mechanistic links and molecular crosstalk are yet to be discovered (Noden and Francis-West, 2006; Sambasivan et al., 2011; Sugii et al., 2017; Ziermann et al., 2018).

Cleft lip with or without cleft palate, which occurs in 1/700 live births, is one of the most common birth defects and significantly affects quality of life (Dixon et al., 2011). The mechanism underlying cleft soft palate is less understood than that of cleft hard palate, but soft palate clefting imposes a significant burden on individuals and healthcare providers, and may require treatment from infancy through adulthood (Wehby and Cassell, 2010). The soft palate is part of the oropharyngeal complex with important functions in swallowing, breathing, hearing and speech, which are disrupted in individuals with clefts. Soft palatal functions are not sufficiently re-established in 30% of cleft patients after surgery (Marrinan et al., 1998; Monroy et al., 2015; Von den Hoff et al., 2018). Owing to the delicate structure of the soft palate, its functional restoration requires long-term multidisciplinary treatment (Monroy et al., 2012).

Studies have identified *Dlx5*, *Fgf10*, *Mn1*, *Tbx22*, *Runx2* and *Twist1* as important regulators of soft palate development (Han et al., 2021; Liu et al., 2008; Sugii et al., 2017). Wnt signaling is of particular interest for further investigation as it is a known mediator of TGF-β signaling during soft palate development (Iwata et al., 2014) but its mechanisms of action in this context have not yet been elucidated. Furthermore, comprehensive screening of expression patterns related to signaling pathways potentially involved in soft palate development indicate that Wnt signaling is predominantly expressed in CNC-derived cells surrounding the myogenic soft palatal cells, making it a strong candidate for mediating communication between them (Janeckova et al., 2019). In general, Wnt signaling is crucial for craniofacial development in humans and mice, and its disruption causes severe craniofacial defects, including cleft palate (Brault et al., 2001; Chen et al., 2009; He et al., 2011; Huelsken et al., 2000; Reynolds et al., 2019). Independently, Wnt signaling has also been shown to play a role during various phases of myogenesis (Suzuki et al., 2018; Zhong et al., 2015).

In the present study, using the soft palate as a model, we highlight how canonical Wnt signaling acts upstream of ciliogenesis. Primary cilia serve as essential mediators of the complex tissue-tissue interactions accompanying soft palate development. We show that persistence of the primary cilia, caused by their dysfunctional disassembly in the CNC-derived mesenchymal cells due to a lack of canonical Wnt signaling, prevents cell cycle progression. This reduces the number of proliferating CNC-derived mesenchymal cells, influences their differentiation status and ultimately results in underdevelopment of the soft palatal muscles. Our study emphasizes the connection between Wnt signaling and ciliogenesis in regulating tissue-tissue interactions to control organogenesis.

Center for Craniofacial Molecular Biology, University of Southern California, Los Angeles, CA 90033, USA.

*Author for correspondence (ychai@usc.edu)

Y.C., 0000-0003-2477-7247

Handling Editor: Liz Robertson
Received 3 August 2022; Accepted 10 February 2023

Development (2023) 150, dev201189. doi:10.1242/dev.201189

RESULTS

Wnt signaling-dependent tissue-tissue interactions are essential for soft palate development

To identify how cell signaling regulates soft palate development, we screened several signaling pathways, including Wnt, Fgf and Hh (Janeckova et al., 2019). Wnt signaling emerged as a strong candidate as it was primarily activated in the CNC-derived mesenchymal cells surrounding the mesoderm-derived myogenic cells during the early development of the soft palate. This corroborated a previously published study, in which it was shown that mesenchymal Wnt signaling mediates TGF-β epithelial signaling to guide myogenesis in the soft palate (Iwata et al., 2014).

To test whether canonical Wnt signaling is functionally required for regulating tissue-tissue interactions in soft palate development, we deleted β-catenin, the key mediator of Wnt signaling, in the CNC-derived mesenchymal cells, without affecting Wnt signaling in epithelial or myogenic cells in *Osr2-Cre;β-catenin*$^{fl/fl}$ mice (Chen et al., 2009) (Fig. 1A,B,E,F). We confirmed efficient reduction of β-catenin expression in the CNC-derived mesenchymal cells (Fig. 1C,D,G,H). In contrast, β-catenin expression was not affected in the epithelial cells, which are not targeted by *Osr2-Cre* (Fig. 1C,D,G,H). Loss of β-catenin in palatal CNC-derived mesenchymal cells resulted in defects in the palatine process of the maxilla and the palatine bone in *Osr2-Cre;β-catenin*$^{fl/fl}$ mice (Fig. 1I, J). Furthermore, the histology revealed complete cleft palate (Fig. 1K, L). The hard palatal shelves failed to grow horizontally towards each other and to fuse together. These phenotypes resulted in postnatal lethality and signified that canonical Wnt signaling in the CNC-derived mesenchymal cells is indispensable for palatogenesis.

We then analyzed the soft palatal defects in *Osr2-Cre;β-catenin*$^{fl/fl}$ mice. The levator veli palatini (LVP) was our focus as the main soft palatal muscle (Monroy et al., 2015). Intraoral whole-mount views and soft tissue CT scans showed complete cleft palate in *Osr2-Cre;β-catenin*$^{fl/fl}$ mice, in comparison with intact well-developed control palates (Fig. 2A-D). Histological analysis further confirmed that the soft palatal shelves were not developed at E18.5 in the *Osr2-Cre;β-catenin*$^{fl/fl}$ mice (Fig. 2E-H). The LVP was significantly affected and no myogenic fibers were detected (Fig. 2I-L). To determine when the muscle phenotype first appears in these mice, we analyzed embryos at different stages and found that the palatal shelf development and the number of MyoD^{+} positive cells at the level of LVP were comparable between controls and mutants at E13.5 (Fig. 2M-P,U), suggesting there were no migration defects affecting the arrival of these myogenic cells at the palatal shelves. The difference in the number of MyoD^{+} positive cells became apparent in *Osr2-Cre;β-catenin*$^{fl/fl}$ mice relative to controls at E14.0 (Fig. 2Q,S,V) and persisted at E14.5 (Fig. 2R,T,W). Therefore, we considered E13.5-E14.0 as the time of phenotype onset, and we used samples at these stages for further analyses.

Wnt signaling is required for the proliferation and cell cycle progression of CNC-derived mesenchymal cells in the soft palate

Balanced cellular activities, such as proliferation and apoptosis, are crucial for mesenchymal cells during soft palate development. In order to determine why soft palatal shelf growth was stunted in *Osr2-Cre;β-catenin*$^{fl/fl}$ mice, we analyzed cellular activities of CNC-derived mesenchymal cells at E13.5 and E14.0, when the

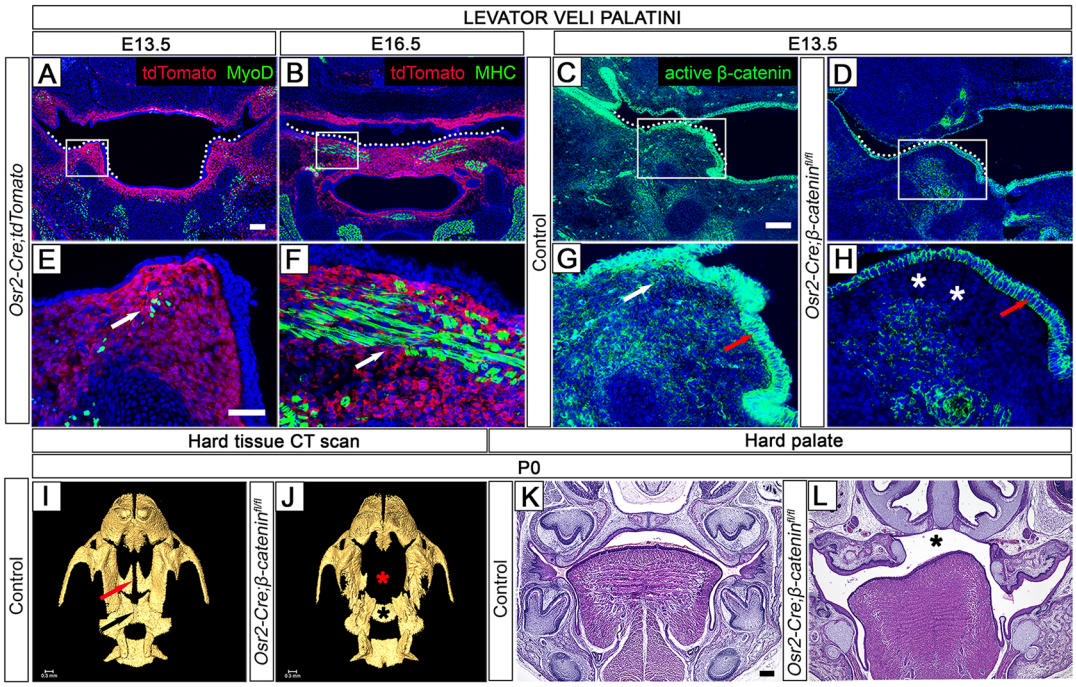

Fig. 1. Wnt signaling from CNC-derived mesenchymal cells is essential for palatogenesis. (A,B,E,F) *Osr2-Cre;tdTomato* mice at E13.5 (A,E) and E16.5 (B,F). (C,D,G,H) Active β-catenin (green) immunofluorescence staining at E13.5 in control (C,G) and *Osr2-Cre;β-catenin*$^{fl/fl}$ (D,H) mice. (I,J) Hard tissue CT scans at P0 showing defects in the palatine process of the maxilla (red asterisk in J) and palatine bone (black asterisk in J) of *Osr2-Cre;β-catenin*$^{fl/fl}$ mice in comparison with the normal palatine process of the maxilla (red arrow in I) and palatine bone (black arrow in I) in controls. (K,L) Hematoxylin and Eosin staining at the level of the hard palate in control (K) and *Osr2-Cre;β-catenin*$^{fl/fl}$ (L) mice at P0. Black asterisk in L identifies the cleft palate in *Osr2-Cre;β-catenin*$^{fl/fl}$. Rectangles in A-D indicate locations of higher magnification images in E-H, respectively. White dotted lines indicate palatal shelves in A-D. White arrows in E-G indicate positive areas in the mesenchyme. Asterisks in H indicate reduced signal in the mesenchyme. Red arrows in G and H indicate positive areas in the epithelium. Scale bars: in A, 100 µm in A and B; in C, 100 µm in C and D; in E, 50 µm in E-H; in I, 0.3 mm in I and J; in K, 200 µm in K and L.

Development (2023) 150, dev201189. doi:10.1242/dev.201189

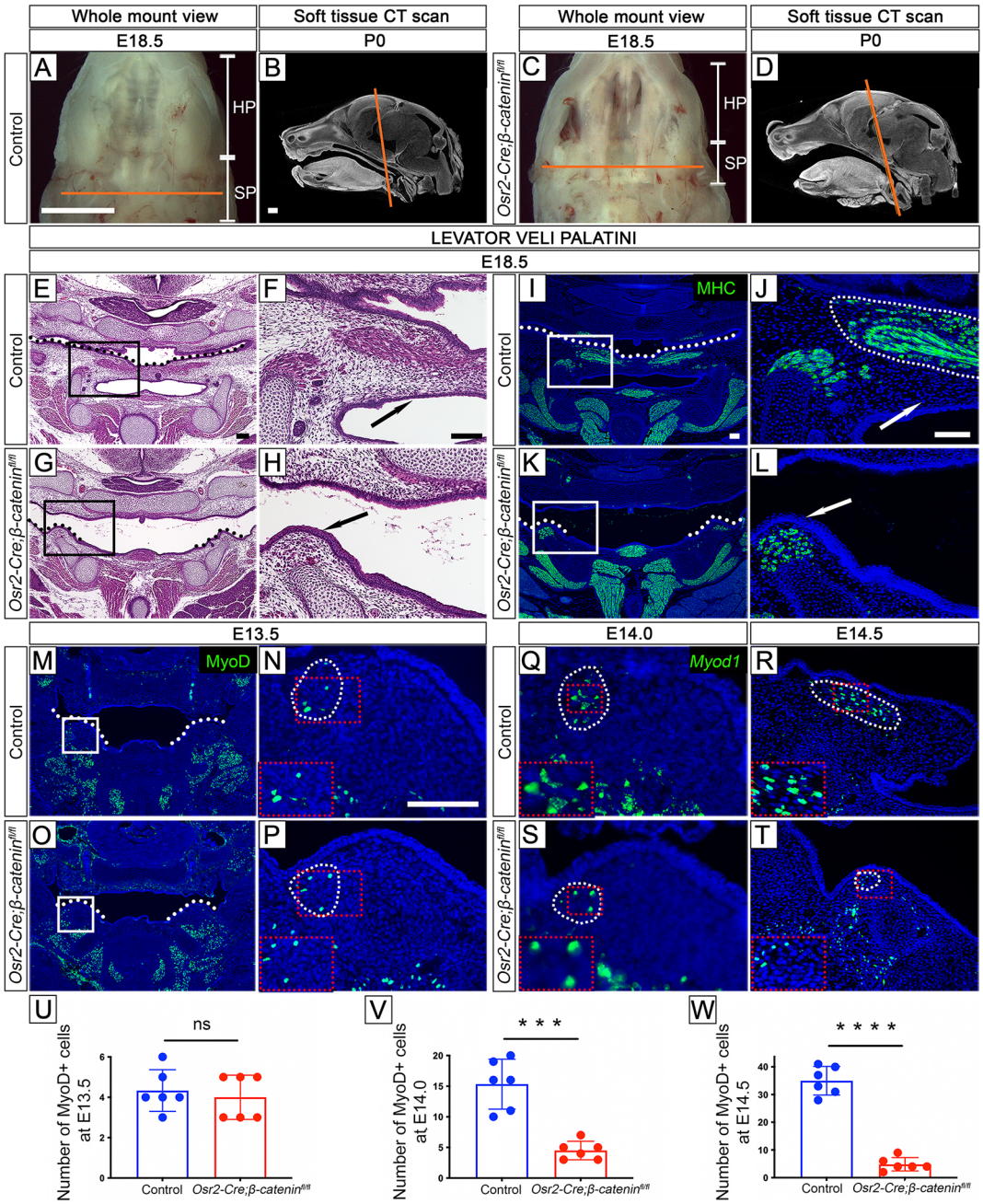

Fig. 2. Wnt signaling from CNC-derived mesenchymal cells is essential for guiding myogenesis through tissue-tissue interactions. (A,C) Intraoral whole-mount views of the maxilla from control (A) and *Osr2-Cre;β-catenin*$^{fl/fl}$ (C) mice at E18.5. (B,D) Soft tissue CT scans at P0 of control (B) and *Osr2-Cre;β-catenin*$^{fl/fl}$ (D) mice. (E-H) Hematoxylin and Eosin staining at the level of the levator veli palatini (LVP) in control (E,F) and *Osr2-Cre;β-catenin*$^{fl/fl}$ (G-H) mice at E18.5. (I-L) MHC (green) immunofluorescence in control (I,J) and *Osr2-Cre;β-catenin*$^{fl/fl}$ (K,L) mice at E18.5. (M-P) MyoD (green) immunofluorescence in control (M,N) and *Osr2-Cre;β-catenin*$^{fl/fl}$ (O-P) mice at E13.5. (Q-T) *Myod1* (green) *in situ* RNAScope hybridization in control (Q,R) and *Osr2-Cre;β-catenin*$^{fl/fl}$ (S,T) mice at E14.0 (Q,S) and E14.5 (R,T). (U-W) Quantification of the number of MyoD^{+} cells at E13.5 (U). ns, not significant; ***P=0.0001 and ****P<0.0001. n=6. Statistical significance was evaluated using an unpaired t-test with two-tailed calculations. Data are mean±s.e.m. Orange lines in A-D indicate positions of the frontal views in E-T. Black and white arrows in F and J indicate the palatal shelves in the control; black and white arrows in H and L indicate the remnants of the soft palatal shelves in *Osr2-Cre;β-catenin*$^{fl/fl}$. Black rectangles in E and G show approximate locations of the higher magnification images in F and H, respectively. White rectangles in I, K, M and O show approximate locations of the higher magnification images in J, L, N, P and Q-T. Red dotted rectangles in N, P and Q-T show the position of the insets in their lower left corners. Black dotted lines in E and G indicate palatal shelves. White dotted lines in I, K, M and O indicate palatal shelves. White dotted lines in J, N, P and Q-T outline the LVP muscle region stained with MHC, MyoD or *Myod1*. Scale bars: in A, 1 mm in A and C; in B, 0.3 mm in B and D; in E, 200 µm in E and G; in F, 100 µm in F and H; in I, 100 µm in I, K, M and O; in J, 100 µm in J, L, R and T; in N, 100 µm in N, P, Q and S.

palatal shelves were still comparable between controls and mutants at the level of the LVP. At this stage, the palatal shelves consisted predominantly of CNC-derived mesenchymal cells with only a few myogenic cells. Our analysis showed decreased proliferation of soft palatal mesenchymal cells in *Osr2-Cre;β-catenin*$^{fl/fl}$ mice at E13.5 (Fig. 3A,B,D,E,I). However, apoptosis was not affected; very few cells were apoptotic in controls or mutants at E13.5 (Fig. 3C,F). To uncover any changes in cell cycle progression between control and

Development (2023) 150, dev201189. doi:10.1242/dev.201189

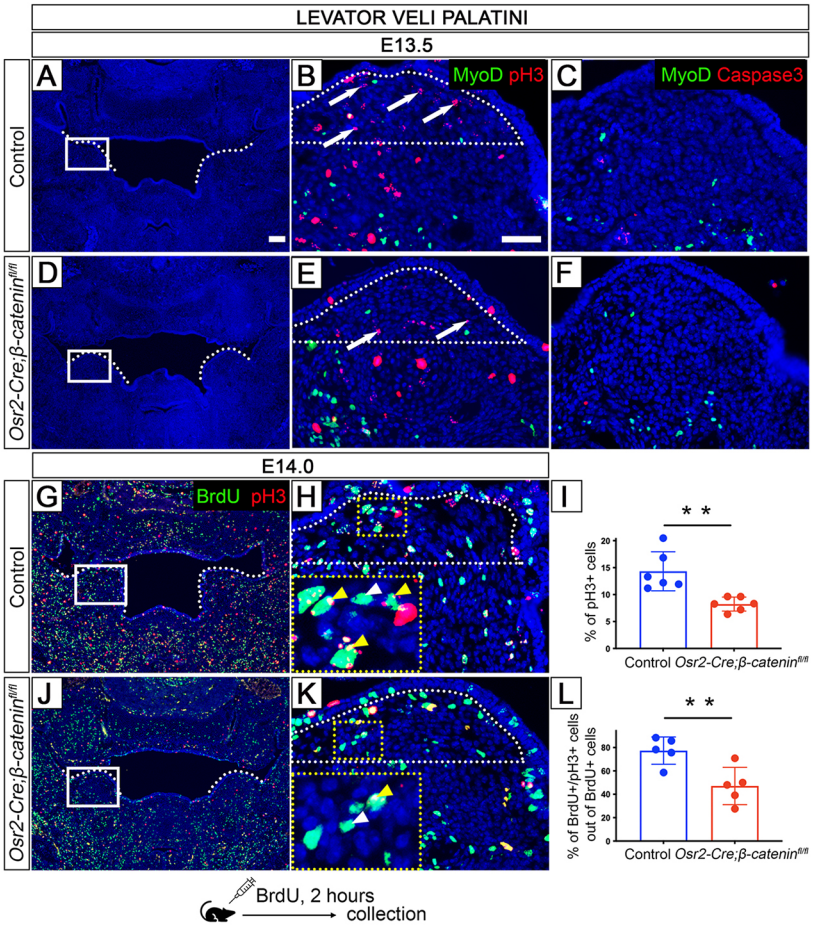

Fig. 3. *Osr2-Cre;β-catenin*$^{fl/fl}$ mice display decreased proliferation of the mesenchymal cells. (A,D) DAPI staining of control (A) and *Osr2-Cre;β-catenin*$^{fl/fl}$ (D) sections at the level of the LVP at E13.5. (B,C,E,F) MyoD (green) and pH3 (red) (B,E), or MyoD (green) and caspase 3 (red) immunofluorescence staining (C,F) in control (B,C) and *Osr2-Cre;β-catenin*$^{fl/fl}$ (E,F) mice. (G,H,J,K) BrdU (green) and pH3 (red) immunofluorescence staining at E14.0 in control (G,H) and *Osr2-Cre;β-catenin*$^{fl/fl}$ (J,K) mice. (I) Quantification of the percentage of pH3-positive cells out of the soft palatal mesenchymal cells outlined by white dotted lines in B and E. $^{**}P$=0.0031. n=6. (L) Quantification of percentage of BrdU$^+$ pH3$^+$ double-positive cells out of total BrdU$^+$ cells in the outlined areas in H and K. $^{**}P$=0.0091. n=5. For I and L, statistical significance was evaluated using an unpaired t-test with two-tailed calculations. Data are mean±s.e.m. Schematic drawing at the bottom indicates the BrdU protocol. White rectangles in A, D, G and J indicate the approximate location of the higher magnification images in B, C, E, F, H and K. White dotted lines in A, D, G and J indicate palatal shelves. White dotted lines in B, E, H and K indicate the area of quantification. Yellow dotted rectangles in H and K indicate the position of the insets in their lower left corners. White arrows in B and E indicate positive signal. White arrowheads in H and K indicate positive cells. Yellow arrowheads in H and K indicate double-positive cells. Scale bars: in A, 100 µm in A, D, G and J; in B, 50 µm in B, C, E, F, H and K.

Osr2-Cre;β-catenin$^{fl/fl}$ mice, we colocalized the S-phase marker BrdU with the M-phase marker pH3 to identify cells that progress from S- to M-phase during the short BrdU labeling. Our analysis revealed fewer BrdU$^+$/pH3$^+$ cells in the palatal shelves of *Osr2-Cre;β-catenin*$^{fl/fl}$ mice at E14.0 (Fig. 3G,H,J,K,L). Therefore, fewer S-phase cells progressed into M-phase in *Osr2-Cre;β-catenin*$^{fl/fl}$ mice. These results indicated that Wnt signaling has a specific role in maintaining appropriate proliferation and cell cycle progression of CNC-derived mesenchymal cells in the soft palate.

Compromised Wnt signaling in mesenchymal cells increases ciliogenesis and decreases myogenesis in the soft palatal region

To uncover how canonical Wnt signaling regulates cell proliferation in the soft palatal mesenchyme, we performed RNA sequencing (RNAseq) analysis of *Osr2-Cre;β-catenin*$^{fl/fl}$ and control mice at E14.0 (Fig. 4A-C) to identify significant changes in the transcriptome and downstream targets in the absence of Wnt signaling in soft palatal mesenchymal cells. We identified significantly affected genes associated with myogenesis and ciliogenesis in the soft palate of *Osr2-Cre;β-catenin*$^{fl/fl}$ samples compared with controls (Fig. 4D). The decrease in soft palatal myogenesis in *Osr2-Cre;β-catenin*$^{fl/fl}$ mice indicated that Wnt signaling in CNC-derived mesenchymal cells is required for myogenic cells through tissue-tissue interactions, consistent with the defects observed in histological analysis (Fig. 2E-L). A striking change in *Osr2-Cre;β-catenin*$^{fl/fl}$ mice was increased ciliogenesis (Fig. 4D). Primary cilia are complex, unique organelles that play an important role in regulating organogenesis and function as cellular antennas (Wheway et al., 2018). The potential involvement of primary cilia in soft palate development has not been explored. To comprehensively validate the ciliary phenotype, we analyzed ciliary structure, intraflagellar transport and post-translational modifications of cilia.

To analyze the ciliary structure in *Osr2-Cre;β-catenin*$^{fl/fl}$ mice, we used γ-tubulin (a marker of the ciliary basal body) and Arl13b (a marker of the ciliary axoneme). We identified increased expression of γ-tubulin and Arl13b in the palatal mesenchyme of *Osr2-Cre;β-catenin*$^{fl/fl}$ mice in comparison with controls (Fig. 4F-N). As cilia are dynamically regulated during cell cycle progression (Kasahara and Inagaki, 2021) and our analysis showed that palatal mesenchymal cells are not progressing to M-phase in *Osr2-Cre;β-catenin*$^{fl/fl}$ mice, we analyzed the RNAseq data with a focus on genes that are essential for ciliary stability and homeostasis (the balance between assembly and disassembly). One of the genes we identified is *Ttll3*, which encodes a glycylase that serves as a post-translational modifier of the ciliary axoneme (Gadadhar et al., 2017). Increased expression of *Ttll3* was confirmed through RNAScope *in situ* staining of soft palatal mesenchyme (Fig. 4O-R). Another post-translational modifier, *Ttll6*, also showed increased expression in the palatal mesenchyme of *Osr2-Cre;β-catenin*$^{fl/fl}$ mice (Fig. S1A-D). Furthermore, we discovered that the expression of *Ift88*, which is involved in ciliary intraflagellar transport, was also increased in the palatal mesenchyme of *Osr2-Cre;β-catenin*$^{fl/fl}$ mice (Fig. 4S-V). In summary, in the absence of canonical Wnt signaling in mesenchymal cells, myogenesis and ciliogenesis are adversely affected in *Osr2-Cre;β-catenin*$^{fl/fl}$ mice.

Development (2023) 150, dev201189. doi:10.1242/dev.201189

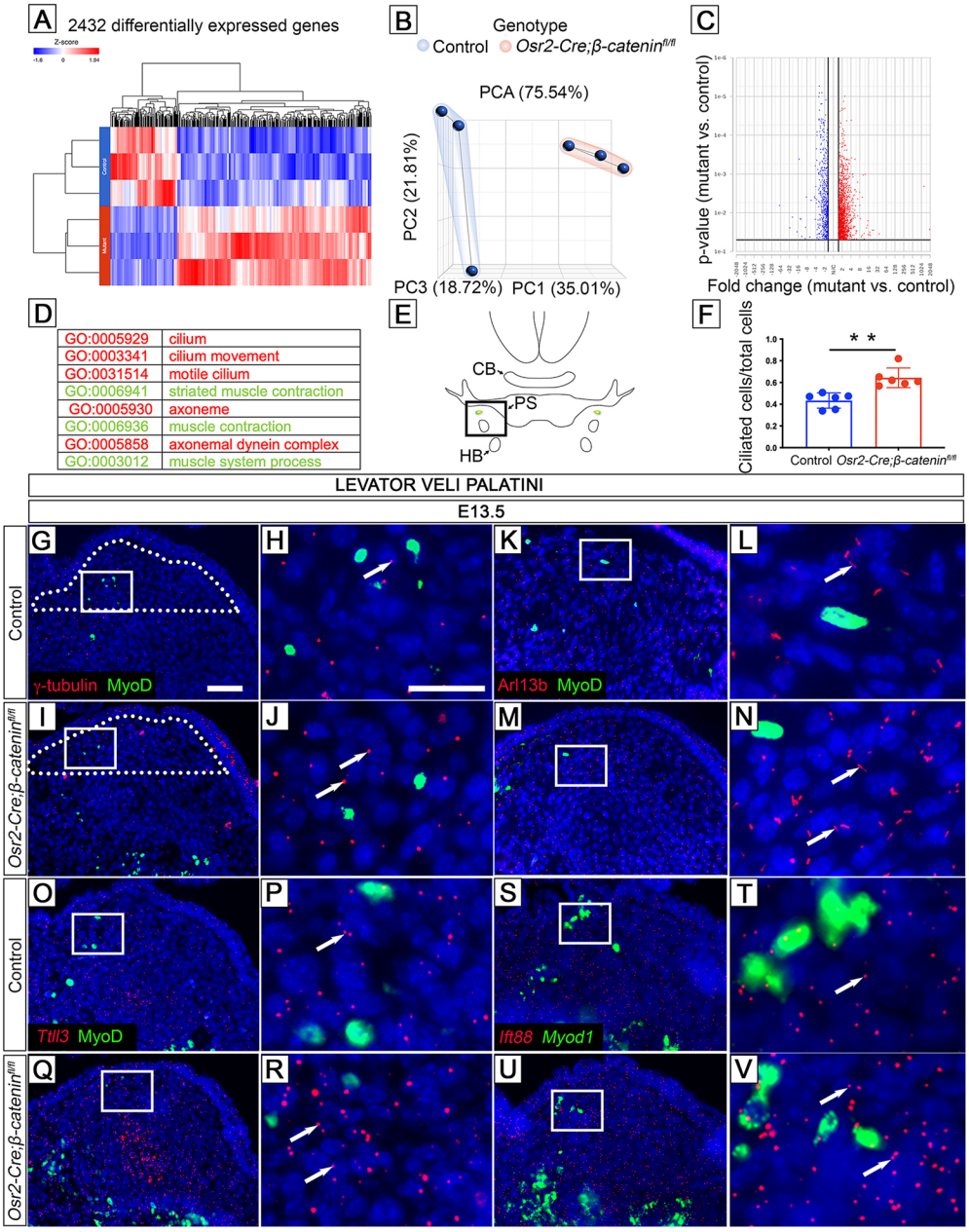

Fig. 4. Loss of Wnt signaling in mesenchymal cells leads to an increase in the number of cilia. (A-C) RNAseq analysis of soft palatal samples from control (blue) and *Osr2-Cre;β-catenin*$^{fl/fl}$ mice (red) collected at E14.0 depicted with heat map (A), PCA plot (B) and volcano plot (C). (D) The most changed GO terms from the Partek Flow analysis indicate changes in muscle (green) and cilium (red). (E) Schematic drawing at the level of the LVP. CB, cranial base; PS, palatal shelf; HB, hyoid bone. (F) γ-Tubulin quantification indicates the percentage of ciliated cells as a ratio of mesenchymal ciliated cells to total number of mesenchymal cells in the areas outlined in G and I. ***P*=0.0012. *n*=6. Statistical significance was evaluated using an unpaired *t*-test with two-tailed calculations. Data are mean ±s.e.m. (G-J) γ-Tubulin (red) and MyoD (green) immunofluorescence staining at E13.5 in control (G,H) and *Osr2-Cre;β-catenin*$^{fl/fl}$ (I,J) mice. (K-N) Arl13b (red) and MyoD (green) immunofluorescence staining at E13.5 in control (K,L) and *Osr2-Cre;β-catenin*$^{fl/fl}$ (M,N) mice. (O-R) *Ttll3* (red) *in situ* RNAScope hybridization and MyoD (green) immunofluorescence staining in control (O,P) and *Osr2-Cre;β-catenin*$^{fl/fl}$ (Q,R) mice. (S-V) *Ift88* (red) and *Myod1* (green) *in situ* RNAScope hybridization in control (S,T) and *Osr2-Cre;β-catenin*$^{fl/fl}$ (U,V) mice. Black rectangle in E shows the approximate location of the images in G, I, K, M, O, Q, S and U. White rectangles in G, I, K, M, O, Q, S and U indicate the areas shown at higher magnification in H, J, L, N, P, R, T and V, respectively. White arrows in H, J, L, N, P, R, T and V indicate the positive signal. Scale bars: in G, 50 µm in G, I, K, M, O, Q, S and U; in H, 20 µm in H, J, L, N, P, R, T and V.

Ttll3 expression is regulated by β-catenin and Tcf7l2

After identifying *Ttll3* as the key factor responsible for dysfunctional ciliary disassembly in *Osr2-Cre;β-catenin*$^{fl/fl}$ mice, we further analyzed this gene. To uncover how *Ttll3* expression is controlled by canonical Wnt signaling, we searched its promoter region for potential binding sites of canonical Wnt-related transcription factors Tcf7, Tcf7l1, Tcf7l2 and Lef1, all of which contain a β-catenin-binding domain (Cadigan and Waterman, 2012). Binding of β-catenin to these transcription factors in the nucleus enables activation or repression of Wnt-responsive genes (Ip et al., 2012; Kim et al., 2017; Ohsugi et al., 2017). Bioinformatic analysis using transcription-binding profiles from the UCSC/JASPAR database showed that Tcf7 and Tcf7l2 can potentially bind to the *Ttll3* promoter region (Fig. 5A), indicating that *Ttll3* may act downstream of canonical Wnt signaling to control ciliary disassembly on mesenchymal cells and ultimately influence soft palate development.

To determine whether Tcf7 or Tcf7l2 presented a better candidate for further analysis, we analyzed our scRNAseq data from E13.5 soft palatal shelves (Fig. 5B) (Han et al., 2021) using the R package SCENIC (Aibar et al., 2017). This allowed us to identify the main genetic regulatory networks (regulons) in early soft palate development to guide identification of the transcription factors that play biological roles in specific clusters identified by scRNAseq (Aibar et al., 2017). Our data revealed that the Tcf7l2 regulon, not that of Tcf7, is present in perimysial cells (Fig. 5C), a population that closely interacts with myogenic progenitor cells during early development of the soft palate and is essential for further myogenesis (Han et al., 2021). These data underscore the importance of canonical Wnt signaling in early soft palate development and point to Tcf7l2 being an important transcription factor during this process. We identified a motif (chr6113388069-113388082) that enables binding of Tcf7l2 to the *Ttll3* promoter region (Fig. 5D). We used a CUT&RUN (cleavage under targets

Development (2023) 150, dev201189. doi:10.1242/dev.201189

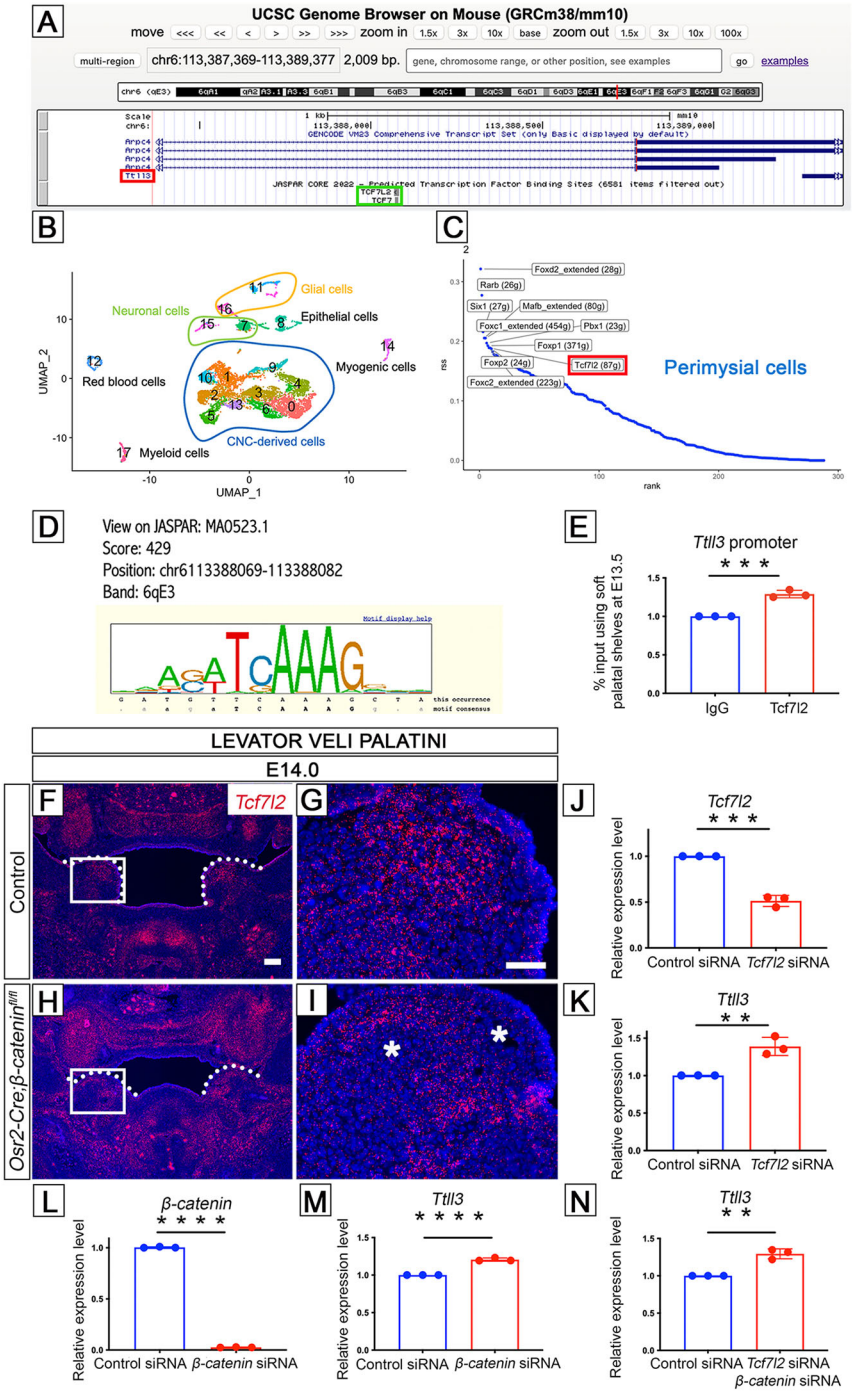

Fig. 5. Wnt signaling directly regulates ciliary genes. (A) Predicted position of Tcf7l2 and Tcf7 binding to the promoter region of *Ttll3* from the UCSC Genome Browser on mouse. Red rectangle marks *Ttll3* and green rectangle highlights Tcf7l2 and Tcf7. (B) UMAP plot of soft palatal cell populations identified by Seurat from E13.5 soft palatal scRNAseq analysis. 0, midline mesenchymal cells; 1, CNC-derived progenitor cells; 2, perimysial cells; 3, osteogenic cells; 4, perimysial cells; 5, chondrogenic cells; 6, mitotic cells; 7, neuronal cells; 8, epithelial cells; 9, perimysial cells; 10, midline mesenchymal cells; 11, glial cells; 12, red blood cells; 13, chondrogenic cells; 14, myogenic cells; 15, neuronal cells; 16, glial cells; 17, myeloid cells. (C) SCENIC analysis of E13.5 soft palatal scRNAseq data shows Tcf7l2 as an important regulon in perimysial cells. Red rectangle highlights Tcf7l2. (D) UCSC binding prediction of the Tcf7l2-binding motif to *Ttll3*. (E) CUT&RUN assay for binding of Tcf7l2 to the *Ttll3* promoter region in the soft palatal tissue at E13.5. ***P=0.0005. (F-I) *Tcf7l2* (red) *in situ* RNAScope hybridization at E14.0 in control (F,G) and *Osr2-Cre; β-catenin$^{fl/fl}$* (H,I) mice. (J-N) qPCR analysis. (J) Efficiency of *Tcf7l2* siRNA (***P=0.0001). (K) Increased expression of *Ttll3* after *Tcf7l2* siRNA treatment (**P=0.0053). (L) Efficiency of β-catenin siRNA (****P<0.0001. (M) Increased expression of *Ttll3* after β-catenin siRNA treatment (****P<0.0001). (N) Increased expression of *Ttll3* after β-catenin and *Tcf7l2* siRNA treatment (**P=0.0015). For E and J-N, statistical significance was evaluated using an unpaired *t*-test with two-tailed calculations. Data are mean±s.e.m. White rectangles in F and H show the approximate location of the higher magnification images in G and I, respectively. White dotted lines indicate palatal shelves in F and H. Asterisks in I show the lack of a positive signal. Scale bars: in F, 100 µm in F and H; in G, 50 µm in G and I.

and release using nuclease) assay (Skene and Honikoff, 2017) and confirmed direct binding of Tcf7l2 to the predicted region at the *Ttll3* promoter site (Fig. 5E). These data suggest that *Ttll3* is a direct target of canonical Wnt signaling in the soft palate, mediated by Tcf7l2.

Next, we examined the expression of *Tcf7l2 in vivo*. *Tcf7l2* was expressed primarily in the palatal mesenchymal cells in controls, and this expression was decreased in *Osr2-Cre;β-catenin$^{fl/fl}$* mice (Fig. 5F-I). To confirm whether Tcf7l2 is responsible for changes in *Ttll3* expression, we performed *in vitro* analysis on primary soft palatal mesenchymal cells isolated from E13.5 control soft palates. Following siRNA-mediated knockdown of *Tcf7l2* in these cells (Fig. 5J), the expression of *Ttll3* was significantly increased (Fig. 5K), suggesting that Tcf7l2 represses *Ttll3* expression in soft palatal mesenchymal cells. In summary, Tcf7l2 can functionally regulate *Ttll3* expression by binding to its promoter.

To support our findings, we used siRNA targeting β-catenin and confirmed its knockdown efficiency (Fig. 5L). Similar to *Tcf7l2* siRNA, decreasing β-catenin caused increased *Ttll3* expression in soft palatal mesenchymal cells (Fig. 5M). Combined knockdown of β-catenin and *Tcf7l2* (β-catenin siRNA:*Tcf7l2* siRNA=1:1) increased *Ttll3* expression (Fig. 5N), similar to β-catenin and *Tcf7l2* alone (Fig. 5K and M), suggesting the collaboration of β-catenin and Tcf7l2 in regulating *Ttll3* expression. Thus, in *Osr2-Cre;β-catenin$^{fl/fl}$* mice, decreased levels of both β-catenin and Tcf7l2 in CNC-derived mesenchymal cells cause stabilization of

Development (2023) 150, dev201189. doi:10.1242/dev.201189

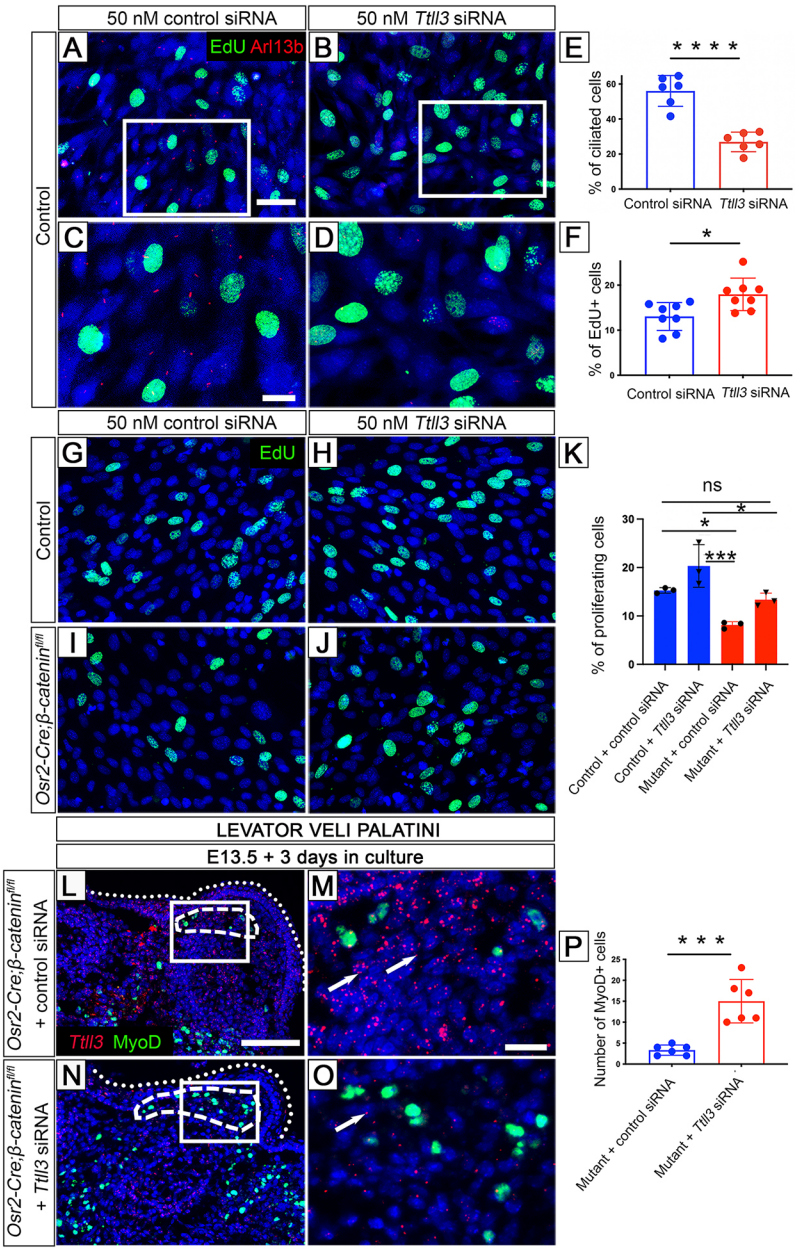

Fig. 6. Dysfunctional ciliary disassembly restrains cell cycle progression of soft palatal cells in *Osr2-Cre;β-catenin$^{fl/fl}$* mice. (A-D) EdU (green) and Arl13b (red) immunofluorescence staining on cells isolated from control mice treated with 50 nM control siRNA (A,C) or 50 nm *Ttll3* siRNA (B,D). (E) Quantification of the percentage of ciliated cells. ****P<0.0001. n=6. (F) Quantification of the percentage of EdU$^+$ cells. *P=0.0112. n=8. (G-J) EdU (green) immunofluorescence staining on cells isolated from control (G,H) and *Osr2-Cre;β-catenin$^{fl/fl}$* (I,J) mice treated with 50 nM control siRNA (G,I) or 50 nm *Ttll3* siRNA (H,J). (K) Quantification of the percentage of EdU$^+$ cells from control and *Osr2-Cre;β-catenin$^{fl/fl}$* (mutant) samples. *P≤0.05, ***P=0.001; ns, not significant. Statistical significance was evaluated using one-way ANOVA. Data are mean±s.e.m. (L-O) *Ttll3* (red) *in situ* RNAScope hybridization and MyoD (green) immunofluorescence staining of *Osr2-Cre;β-catenin$^{fl/fl}$* samples injected with control (L,M) or *Ttll3* (N,O) siRNA. (P) Quantification of MyoD$^+$ cells in *Osr2-Cre;β-catenin$^{fl/fl}$* (mutant) samples injected with control or *Ttll3* siRNA. ***P=0.0003. n=6. For E, F and P, statistical significance was evaluated using an unpaired *t*-test with two-tailed calculations. Data are mean±s.e.m. White rectangles in A, B, L and N indicate the approximate locations of the higher magnification images in C, D, M and O, respectively. White dotted lines in L and N indicate palatal shelves. White dashed lines outline the LVP muscle region stained for MyoD in L and N. Scale bars: in A, 50 µm in A, B and G-J; in C, 20 µm in C and D; in L, 100 µm in L and N; in M, 20 µm in M and O.

cilia and prevent these cells from progressing through the cell cycle, whereas, in normal conditions, β-catenin and Tcf7l2 are able to repress *Ttll3* for ciliary homeostasis. These results reveal the mechanism by which Wnt signaling regulates the precise balance of ciliary assembly and disassembly that is indispensable for soft palate development.

Ciliary assembly restrains cell cycle progression in soft palatal mesenchymal cells

Our results suggest that the disturbed cell cycle progression of the palatal mesenchymal cells in *Osr2-Cre;β-catenin$^{fl/fl}$* mice is caused by dysfunctional ciliary disassembly, disrupting ciliary homeostasis. Therefore, we hypothesized that restoring the ciliary homeostatic balance could rescue cell proliferation in the soft palate of *Osr2-Cre;β-catenin$^{fl/fl}$* mice. To test this hypothesis, we treated soft palatal mesenchymal cells isolated from *Osr2-Cre;β-catenin$^{fl/fl}$* mice with *Ttll3* siRNA and observed a decrease in ciliated cells, as shown by reduced staining of ciliary axonemes by Arl13b (Fig. 6A-E). This treatment also increased proliferation of CNC-derived soft palatal cells (Fig. 6A-D,F), suggesting that ciliary assembly can restrain their cell cycle progression. Moreover, *Ttll3* siRNA treatment restored proliferation of CNC-derived palatal mesenchymal cells from *Osr2-Cre;β-catenin$^{fl/fl}$* mice to a level comparable with that of controls (Fig. 6G-K).

Furthermore, to investigate whether reducing *Ttll3* expression could rescue the myogenic defect in *Osr2-Cre;β-catenin$^{fl/fl}$* mice, we optimized an *in vitro* system to culture 300 µm slices of embryonic heads (Feng et al., 2022) and microinjected *Ttll3* siRNA into *Osr2-Cre;β-catenin$^{fl/fl}$* soft palatal shelf mesenchyme to restore the *Ttll3* expression level. After 3 days in culture, we confirmed that *Ttll3* expression decreased following *Ttll3* siRNA microinjection in comparison with control siRNA (Fig. 6L-O). We observed an increase of MyoD$^+$ cells in *Osr2-Cre;β-catenin$^{fl/fl}$* samples injected with *Ttll3* siRNA in comparison with *Osr2-Cre;β-catenin$^{fl/fl}$* samples that were injected with control siRNA (Fig. 6L-P). Collectively, these results indicate that strict control of ciliary

Development (2023) 150, dev201189. doi:10.1242/dev.201189

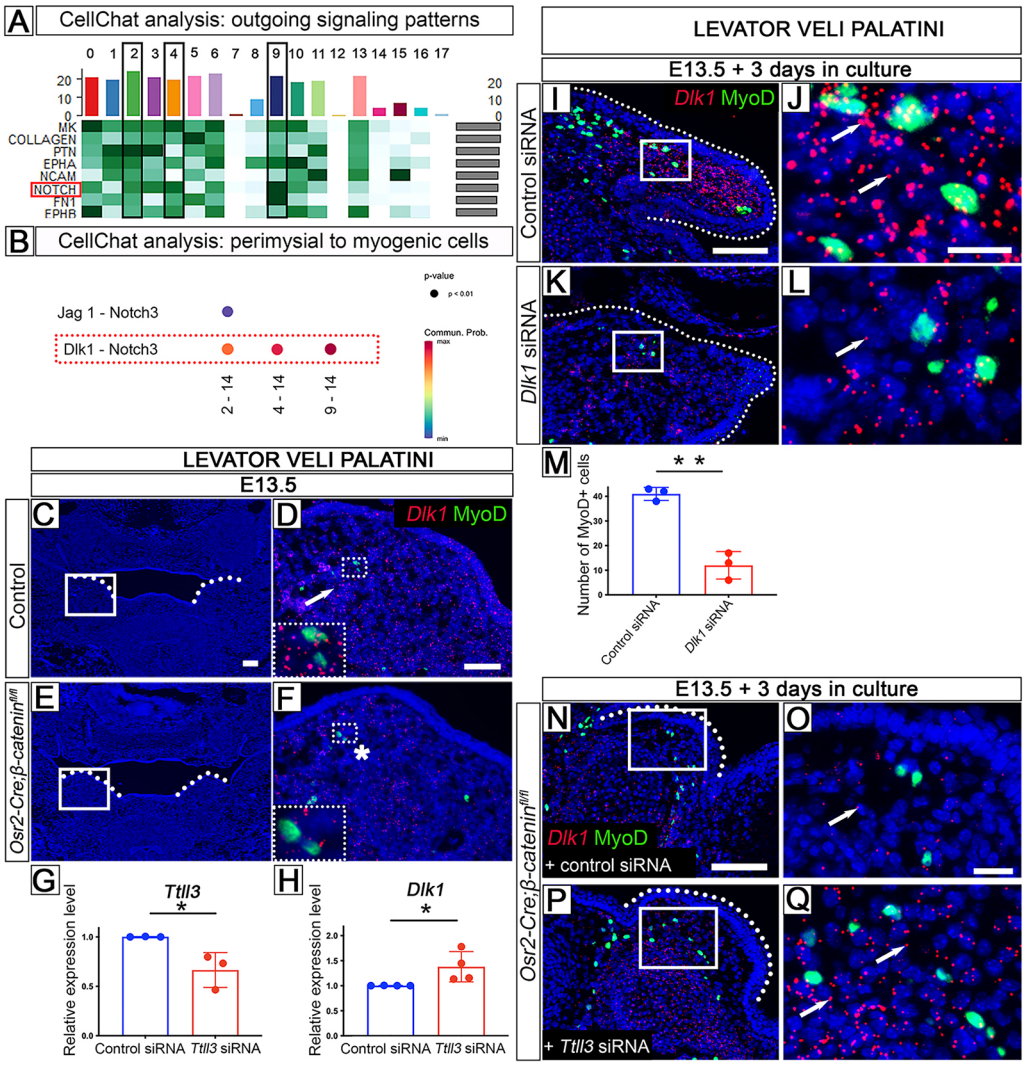

Fig. 7. Primary cilia influence soft palate muscle development by regulating the perimysial fate of CNC-derived palatal mesenchyme cells, which further disrupts soft palate myogenesis. (A) CellChat analysis of E13.5 soft palatal scRNAseq data showing a heatmap visualizing outgoing signaling patterns. 0, midline mesenchymal cells; 1, CNC-derived progenitor cells; 2, perimysial cells; 3, osteogenic cells; 4, perimysial cells; 5, chondrogenic cells; 6, mitotic cells; 7, neuronal cells; 8, epithelial cells; 9, perimysial cells; 10, midline mesenchymal cells; 11, glial cells; 12, red blood cells; 13, chondrogenic cells; 14, myogenic cells; 15, neuronal cells; 16, glial cells; 17, myeloid cells. Red rectangle highlights Notch signaling and black rectangles mark perimysial clusters (2, 4 and 9). (B) Notch signaling activity is shown in the direction of perimysial to myogenic cells (2→14, 4→14 and 9→14). Red dotted rectangle highlights Dlk1/Notch3. (C-F) *Dlk1* (red) *in situ* RNAScope hybridization and MyoD (green) immunohistochemistry at E13.5 in control (C,D) and *Osr2-Cre;β-catenin*$^{fl/fl}$ (E,F) mice. (G,H) qPCR analysis. Efficiency of *Ttll3* siRNA. **P*=0.0297 (G). Increased expression of *Dlk1* after *Ttll3* siRNA treatment. **P*=0.0477. *n*=4 (H). (I-L) *Dlk1* (red) *in situ* RNAScope hybridization and MyoD (green) immunofluorescence staining of control samples injected with control (I,J) or *Dlk1* (K,L) siRNA. (M) Quantification of MyoD^{+} cells in control samples injected with control or *Dlk1* siRNA. ***P*=0.0012. For G, H and M, statistical significance was evaluated using an unpaired *t*-test with two-tailed calculations. Data are mean±s.e.m. (N-Q) *Dlk1* (red) *in situ* RNAScope hybridization and MyoD (green) immunofluorescence staining of *Osr2-Cre;β-catenin*$^{fl/fl}$ samples injected with control (N,O) or *Ttll3* (P,Q) siRNA. White rectangles in C, E, I, K, N and P show the approximate location of the higher magnification images in D, F, J, L, O and Q, respectively. White dotted rectangles in D and F show the position of the insets in their lower left corners. White dotted lines indicate palatal shelves in C, E, I, K, N and P. White arrows in D, J, L, O and Q indicate positive signal. Asterisk in F indicates the lack of positive signal. Scale bars: in C, 100 µm in C and E; in D, 50 µm in D and F; in I, 100 µm in I and K; in J, 20 µm in J and L; in N, 100 µm in N and P; in O, 20 µm in O and Q.

homeostasis is essential for proper proliferation, cell cycle progression of CNC-derived mesenchymal cells and development of the soft palate muscles.

Primary cilia regulate the perimysial fate of CNC-derived palatal mesenchymal cells

To discover the mechanism of communication among CNC-derived mesenchymal and myogenic cells, we analyzed our E13.5 soft palatal scRNAseq data (Han et al., 2021) because the altered cell proliferation phenotype in *Osr2-Cre;β-catenin*$^{fl/fl}$ mice appears immediately after this stage. We used CellChat to identify predicted ligand-receptor interactions between the CNC-derived mesenchymal and myogenic cells (Jin et al., 2021). Among the highly ranked predicted outgoing signaling patterns from the perimysial cells (clusters 2, 4 and 9) was Notch signaling (Fig. 7A), especially the Dlk1/Notch3 ligand and receptor combination (Fig. 7B), which represents non-canonical Notch signaling that could be received by the myogenic cells. Supporting this notion, we found decreased expression of *Dlk1* in the palatal mesenchyme of *Osr2-Cre;β-catenin*$^{fl/fl}$ mice (Fig. 7C-F). As primary cilia function

Development (2023) 150, dev201189. doi:10.1242/dev.201189

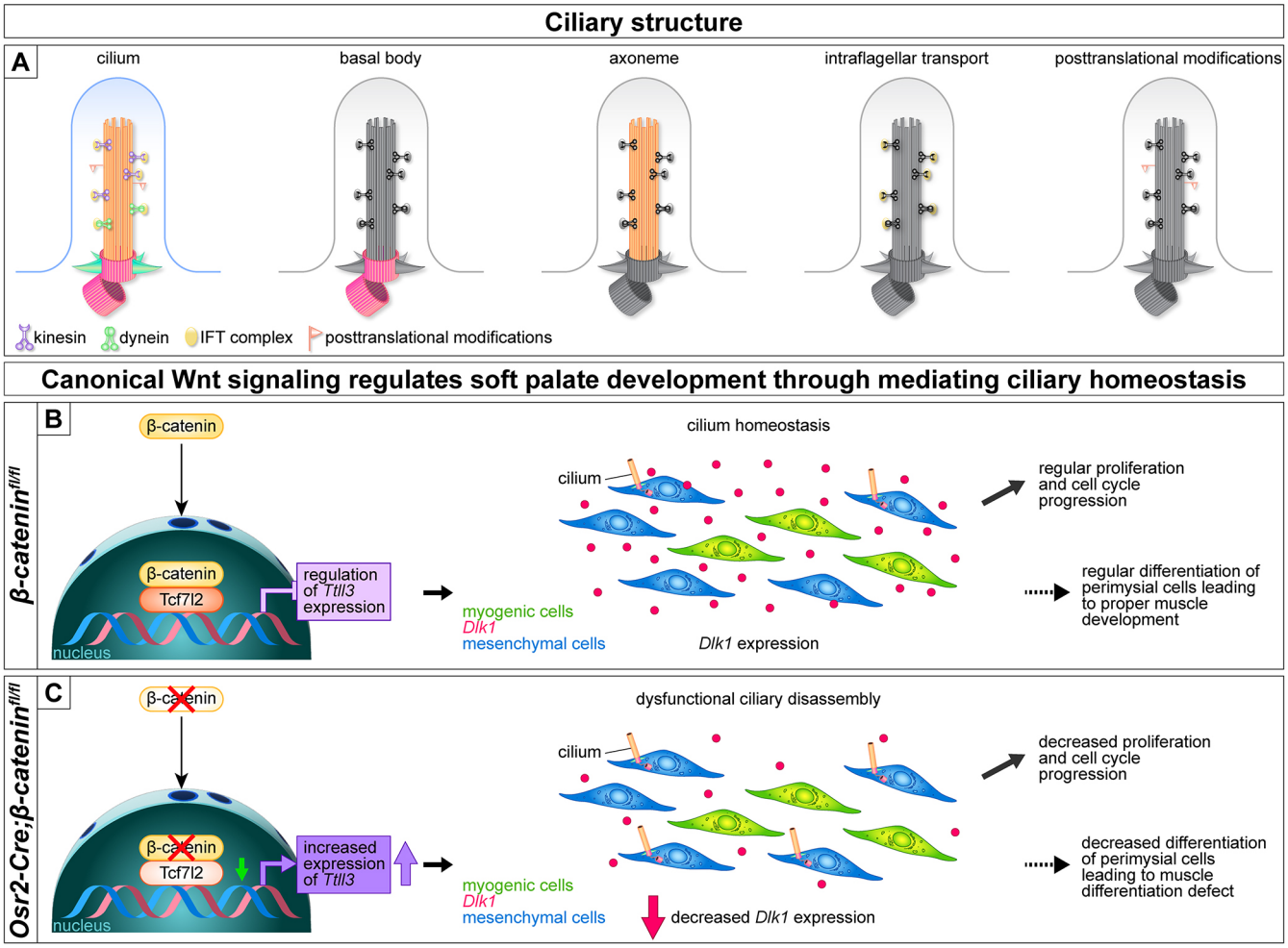

Fig. 8. Loss of Wnt signaling in mesenchymal cells leads to disruption of ciliary homeostasis and defective muscle development. (A) Schematic drawings of primary cilia focusing on structure (basal body and ciliary axoneme), intraflagellar transport and post-translational modifications. (B) In control mice, stabilized β-catenin translocates to the nucleus and regulates *Ttll3* expression through *Tcf7l2*, which maintains ciliary homeostasis, regular proliferation, cell cycle progression and differentiation of perimysial cells. This ultimately results in proper development of the soft palatal muscles. (C) In *Osr2-Cre; β-catenin*$^{fl/fl}$ mice, deletion of β-catenin from CNC-derived mesenchymal cells causes decreased expression of *Tcf7l2* and increased expression of *Ttll3*, which leads to dysfunctional ciliary disassembly, decreased proliferation and cell cycle progression of perimysial cells. As a result, we observe decreased *Dlk1* expression and defective soft palatal muscle development.

as a signaling hub, we hypothesized that, apart from influencing the cell cycle and its progression, primary cilia could also be responsible for the differentiation status of the perimysial cells that are essential for the development of soft palatal muscles. Furthermore, in our scRNAseq analysis, *Dlk1* was identified as one of the top three molecules enriched in the perimysial cells, and it can function both as a transmembrane and secreted protein, making it a good candidate for mediating the communication among CNC-derived mesenchymal and myogenic cells (Feng et al., 2022). After sufficiently decreasing the expression of *Ttll3* using siRNA in the primary soft palatal mesenchymal cells *in vitro* (Fig. 7G), we observed increased expression of *Dlk1* (Fig. 7H). These findings are consistent with our *in vivo* finding that overexpression of *Ttll3* caused a decrease in *Dlk1* expression.

To identify the functional requirement of *Dlk1* for the myogenesis of the LVP, we also used the *in vitro* slice culture system (Feng et al., 2022) to culture slices from E13.5 control embryonic heads containing the LVP, followed by microinjection of control or *Dlk1* siRNA. Although the MyoD^{+} precursors for LVP continued to develop in the soft palatal shelf injected with control siRNA (Fig. 7I-J), the number of MyoD^{+} precursors did not increase in the palatal shelves following *Dlk1* siRNA treatment (Fig. 7K-M). Furthermore, the *Dlk1* expression was restored in *Osr2-Cre; β-catenin*$^{fl/fl}$ slice cultures injected with *Ttll3* siRNA in comparison with those injected with control siRNA (Fig. 7N-Q), corresponding to a rescue of the number of MyoD^{+} cells (Fig. 6P). These experiments demonstrate that *Ttll3* expression regulates the expression of *Dlk1* in the soft palatal mesenchymal cells and ultimately myogenesis through cell-cell interaction. Therefore, in the soft palate, the homeostasis of primary cilia influenced by canonical Wnt signaling coordinates both the proliferation and cell cycle progression of the CNC-derived mesenchymal cells as well as the differentiation of perimysial cells, which ultimately drives soft palatal myogenesis (Fig. 8).

DISCUSSION

The soft palate is an essential part of the oropharyngeal complex, fulfilling vital functions, including breathing, hearing, swallowing and speech, all of which are affected in individuals with cleft palate (Monroy et al., 2015). Cleft soft palate is less commonly studied

Development (2023) 150, dev201189. doi:10.1242/dev.201189

than cleft hard palate, yet it accompanies the majority of cleft cases, and functional restoration of the soft palatal tissue has a low surgical success rate (Monroy et al., 2015; Von den Hoff et al., 2018). Moreover, it imposes a significant burden on patients, families and healthcare providers, as multidisciplinary treatment may be required into adulthood (Von den Hoff et al., 2018). Clinically, individuals with soft palatal clefts exhibit a reduced number of myogenic cells, together with misorientation, lack of fusion, misalignment, atrophy and fibrosis of the soft palatal muscles (Li et al., 2019; Monroy et al., 2015). The detailed molecular mechanisms involved in regulating soft palate development still need to be elucidated, including the reciprocal interactions among the CNC-derived mesenchymal cells, mesoderm-derived myogenic cells, ectoderm-derived epithelial cells and mediators of these communication channels, such as the secreted factors conveying the message or special organelles that may be involved (Li et al., 2019). A better understanding of these signaling mechanisms may contribute to the development of improved, biologically informed soft palatal muscle restoration strategies.

After screening for expression patterns of several signaling pathways, we uncovered that Wnt signaling is activated primarily in the CNC-derived mesenchymal cells surrounding the myogenic cells during soft palatal muscle development. Although mutations in Wnt signaling genes are well described in orofacial clefting in humans, as well as mice, and this pathway is independently known to play a role in regulating myogenesis, here, we have focused on its function in the soft palate (Reynolds et al., 2019; Suzuki et al., 2018). Studying Wnt signaling in murine palatogenesis is otherwise very challenging due to embryonic lethality and failure of craniofacial development after conditional deletion of β-catenin using the more broadly expressed *Wnt1-Cre* driver (Brault et al., 2001). In the current study, loss of canonical Wnt signaling only in the CNC-derived palatal mesenchymal cells using the *Osr2-Cre* mouse model created an opportunity to study the role of Wnt signaling in regulating tissue-tissue interactions during soft palate development.

We discovered that canonical Wnt signaling is essential for proper soft palatal muscle development, and in particular, its regulation of ciliogenesis is indispensable for the proliferation, cell cycle progression and differentiation of CNC-derived mesenchymal cells. These findings agree with previously published data establishing that cilia must disassemble before cells enter the M phase of the cell cycle; otherwise, they function as a cell cycle brake (Liu et al., 2021). Indeed, in *Osr2-Cre;β-catenin*$^{fl/fl}$ mice, the CNC-derived mesenchymal cells do not progress into M phase and exhibit increased expression of *Ttll3*, which encodes a glycylase required for ciliary stability (Gadadhar et al., 2017). Restoring ciliary homeostasis by knocking down expression of *Ttll3* rescues these cellular defects in CNC-derived mesenchyme and ultimately rescues myogenesis in *Osr2-Cre;β-catenin*$^{fl/fl}$ mice. Canonical Wnt signaling therefore influences ciliary post-translational modifications and disassembly, cell cycle progression of the CNC-derived mesenchymal cells, and consequently soft palatal muscle development through cell-cell interactions.

As canonical Wnt signaling is a complex pathway, it is important to determine which of its mediators is the furthest downstream, such that it can bind with β-catenin to directly regulate the expression of ciliary genes. Transcription factors Tcf7, Tcf7l1, Tcf7l2 and Lef1 each contain a β-catenin-binding domain and this binding determines the specificity of canonical Wnt signaling in activating or repressing canonical Wnt-responsive genes in various tissues and organs (Cadigan and Waterman, 2012; Ip et al., 2012; Kim et al., 2017; Ohsugi et al., 2017). We discovered that both β-catenin and Tcf7l2 can regulate genes related to ciliogenesis, which play important roles in regulating the integrity of the soft palatal shelves and muscle development. Moreover, Tcf7l2 is an important regulon in perimysial cells, further supporting the importance of canonical Wnt signaling in early soft palate development. These data are consistent with the previously reported role of Tcf7l2-mediated canonical Wnt signaling in early embryonic limb muscle development (Kardon et al., 2003). In addition, TGF-β-mediated reduction of Tcf7l2 occurs in the mesenchymal stromal cells but not in myoblasts, also supporting the role of Tcf7l2 in cells surrounding the muscle cells during myogenesis (Contreras et al., 2020).

Intriguingly, the relationship between Wnt signaling and ciliogenesis is unclear. To date, limited studies have reported Wnt signaling being upstream of ciliogenesis. It has been shown, on the basis of Kupffer's vesicle motile cilia in zebrafish (Caron et al., 2012) and *in vitro* experiments on human telomerase reverse transcriptase-immortalized retinal pigment epithelial cells (Kyun et al., 2020), that Wnt stimulation promotes primary ciliogenesis. The effects of cilia on Wnt signaling in the reverse direction are uncertain. After manipulating cilium-related genes, Wnt signaling may be restricted (Corbit et al., 2008) or unchanged (Ocbina et al., 2009), and it has also been proposed that cilia serve as a switch between canonical and non-canonical Wnt signaling (Simons et al., 2005). Our study sheds light on the intricate relationship between Wnt signaling and ciliogenesis. We demonstrate the direct involvement of the Wnt signaling pathway in the regulation of ciliary genes during soft palate development.

Furthermore, we discovered a previously unappreciated role of primary cilia in regulating soft palate development. Several studies have reported craniofacial phenotypes, including cleft palate, that are associated with ciliopathies, especially Joubert syndrome, Meckel-Gruber syndrome, Oro-facial-digital syndrome and Ellis-van Creveld syndrome (Brugmann et al., 2010b; Schock and Brugmann, 2017). Analysis of Arl13, which marks the ciliary axoneme, indicated an increased number of cilia in CNC-derived soft palatal mesenchymal cells in *Osr2-Cre;β-catenin*$^{fl/fl}$ mice and its mutation is linked to Joubert syndrome that manifests with cleft palate (Cantagrel et al., 2008; Caspary et al., 2007; Poretti et al., 2012). Primary cilia have been shown to play a role in regulating hard palate development (*Ift88*, *Kif3a* and *Tmem107*) and skeletal muscle development (Brugmann et al., 2010a; Fu et al., 2014; Tian et al., 2017), but whether they are involved in soft palate development has not been reported. Our study highlights primary cilia as key mediators of soft palatal muscle development.

Cilia have also been suggested as key regulators for cell-cell interactions (Wang and Barr, 2018). Our analysis has shown that there is strict interdependence of individual signals and collective corresponding cellular responses, with primary cilia serving as the integration hub. Previously, cilia have been identified as key for maintaining the balance between proliferation and differentiation, e.g. in kidney epithelial cells; they fulfil this function through paracrine signaling (Boletta et al., 2000; Irigoin and Badano, 2011). In our model, primary cilia influence both the proliferation and differentiation of CNC-derived mesenchymal cells to establish and maintain interactions with myogenic cells during morphogenesis. In this study, Notch signaling has been identified as one of the top enriched signaling pathways involved in interactions between perimysial-derived signaling molecules communicating with the myogenic cells in soft palate development. Moreover, *Dlk1* is one of the top three molecules enriched in palatal perimysial cells (Feng

Development (2023) 150, dev201189. doi:10.1242/dev.201189

et al., 2022). We found decreased expression of *Dlk1* in the soft palate of *Osr2-Cre;β-catenin*$^{fl/fl}$ mice, suggesting changes in differentiation of perimysial cells. These changes ultimately lead to defective palatal muscle development. Our data agree with previously published work supporting the role of *Dlk1* in skeletal muscle development and regeneration (Shin et al., 2014; Waddell et al., 2010).

Overall, our study points to the complexity and combination of signaling pathways, cellular processes and their interaction with organelles, such as cilia, coming together to orchestrate embryonic development of the soft palatal region. Canonical Wnt signaling influences the proliferation and ciliary homeostasis of soft palatal mesenchymal cells, enabling their differentiation and ultimately promoting proper muscle development. Our study describes primary cilia as the missing mechanistic link that relays diverse signals from CNC-derived mesenchymal cells to myogenic cells to enable the congruency of the whole system, including the interactions that initiate sustained differentiation of the CNC-derived mesenchymal cells and their functional diversity. These results represent important findings that ultimately will lead to more effective functional muscle restoration for individuals with orofacial clefts.

MATERIALS AND METHODS

Animals and embryo collection

All animal handling was performed according to federal regulations with approval from the Institutional Animal Care and Use Committee (IACUC) at the University of Southern California (protocol 9320). C57BL/6J mice (Jackson Laboratory, 000664) were used for this study. *Osr2-CreKI* mice (Chen et al., 2009) (a gift from Rulang Jiang, Cincinnati Children's Hospital, OH, USA) were crossed with *β-catenin*$^{fl/fl}$ (Brault et al., 2001) (Jackson Laboratory, 004152) and *tdTomato* conditional reporter mice (Jackson Laboratory, 007905) to generate *Osr2-Cre;β-catenin*$^{fl/+}$ males or *Osr2-Cre;tdTomato*$^{fl/+}$ embryos. The *Osr2-Cre;β-catenin*$^{fl/+}$ males were further crossed with *β-catenin*$^{fl/fl}$ females to generate *Osr2-Cre;β-catenin*$^{fl/fl}$ embryos. As control samples, either *β-catenin*$^{fl/+}$ or *β-catenin*$^{fl/fl}$ were used. Pregnant females were euthanized by carbon dioxide overdose followed by cervical dislocation. Embryos (regardless of their sex) were collected at various developmental stages [embryonic day (E) 13.5, E14.0, E14.5 and E18.5, and postnatal day (P)0] and fixed overnight in 10% neutral buffered formalin solution (Sigma-Aldrich, HT501128). E18.5 and P0 samples were decalcified in ethylenediaminetetraacetic acid [EDTA (pH 7.1-7.3), Alfa Aesar, A15161) for 1 week and processed for cryosectioning or paraffin wax embedding and sectioning (8 µm).

MicroCT analysis

MicroCT scans of P0 *β-catenin*$^{fl/fl}$ and *Osr2-Cre;β-catenin*$^{fl/fl}$ mice were obtained from a SCANCO mCT50 scanner at the University of Southern California Molecular Imaging Center with the X-ray source at 70 kVp and 114 mA, and all the data were collected at a resolution of 10 mM.

Histological staining and immunofluorescence

Paraffin wax-embedded sections were used for Hematoxylin and Eosin staining. The histological protocol is described in detail in our previous publication (Janeckova et al., 2019). For immunohistofluorescence, cryosections were air-dried at room temperature and then at 37°C for 15 min each. Distilled water was used for removing OCT (5 min wash) and slides were treated with 3% hydrogen peroxide solution (10 min), citrate-based antigen unmasking solution (Vector, H-3300-250) for 15 min at 99°C, blocking reagent (Thermo Fisher Scientific, B40922) for 1 h at room temperature and primary antibody overnight, followed by washes in PBST. Incubation with secondary antibody was performed for 2 h at room temperature with three subsequent washes in PBST and final counterstaining with DAPI (Thermo Fisher Scientific, D1306) for 5 min. Primary antibodies used in this study were as follows: rabbit monoclonal active β-catenin (Cell Signaling Technology, 19807S, 1:100 with TSA), mouse monoclonal, myosin heavy chain, MHC (DSHB, MF20, 1:10), rabbit polyclonal anti-phospho-histone H3, pH3 (Sigma-Aldrich, 06-570, 1:100), rabbit monoclonal cleaved caspase 3 (Cell Signaling Technology, 9664S, 1:100), rabbit monoclonal MyoD (Abcam, ab133627, 1:200 with TSA), rabbit polyclonal γ-tubulin (Sigma-Aldrich, T5192, 1:100), rabbit polyclonal Arl13b (Proteintech, 17711-1-AP, 1:100), rabbit polyclonal red fluorescein protein, RFP (Rockland, 600-401-379, 1:500 with TSA) and rat monoclonal BrdU (Abcam, ab6326, 1:100). The following secondary antibodies were used in this study: Alexa Fluor 488 anti-mouse (Thermo Fisher Scientific, A11001, 1:200), Alexa Fluor 568 anti-rabbit, (Thermo Fisher Scientific, A11011, 1:200) and anti-rabbit HRP (Vector Laboratories, PI-1000, 1:200) (Table S1). For active β-catenin, MyoD and RFP immunostaining, TSA Plus FITC or Cy3 (Akoya Bioscience, NEL7744001KT or NEL771B001KT) was applied for 3 min before DAPI counterstaining.

RNAScope

Cryosections were air dried at room temperature and at 37°C for 15 min each. Distilled water was used for removing the OCT (5-min wash) and slides were treated with a pre-heated target retrieval reagent (Advanced Cell Diagnostics, ACD, 322000) for 15 min at 99°C. Standard RNAScope reagents were used according to the manufacturer's instructions using RNAScope Multiplex Fluorescent Detection Kit v2 (Advanced Cell Diagnostics, 323110). The following probes from Advanced Cell Diagnostics were used in this study: Mm-*Myod1* (316081), Mm-*Ttll3* (586791), Mm-*Ttll6* (570931), Mm-*Ift88* (420211), Mm-*Tcf7l2* (466901) and Mm-*Dlk1* (405971).

BrdU and EdU incorporation and staining

A short 2 h pulse injection of BrdU (500 µg per 10 g body weight) was administered intraperitoneally at E14.0 to *β-catenin*$^{fl/fl}$ and *Osr2-Cre;β-catenin*$^{fl/fl}$ mice. EdU (10 mg/1 ml PBS) was used on cell cultures for 2 h before the fixation of the cells overnight in 10% neutral buffered formalin solution (Sigma-Aldrich, HT501128). EdU was visualized using a Click-iT Plus EdU Cell Proliferation Kit (Thermo Fisher Scientific, C10637) followed by DAPI staining (Thermo Fisher Scientific, D1306, 5 min).

RNA sequencing and qPCR analysis

The posterior part of the secondary palate (last third of the secondary palate, i.e. the region of the soft palate) was dissected into RNALater (Thermo Fisher Scientific, AM7020). Samples were stored at −80°C, and when sufficient control and mutant samples were obtained (minimum of n=3 per genotype), RNeasy Plus Micro Kit (Qiagen, 74034) was used to isolate RNA. UCLA Technology Center for Genomics and Bioinformatics performed determination of the RNA quality and subsequent cDNA library preparation and sequencing (single-end reads with 75 cycles, Illumina Nextseq 500 platform). Differential expression was calculated by selecting transcripts with fold change ≤ -1.5 or ≥ 1.5 and a significance level of P <0.05 using PartekFlow. The RNA sequencing data generated in this study have been deposited in GEO (Edgar et al., 2002) under accession number GSE208619. The soft palatal tissue was also used for primary cell culture followed by qPCR analysis; after RNA isolation, cDNA was transcribed using an iScript cDNA Synthesis Kit (Bio-Rad, 1708891). The qPCR reaction was run using SsoFast EvaGreen Supermix (Bio-Rad, 172-5202) on a Bio-Rad CFX96 Real-Time System. Values were normalized to *Gapdh* using the $2^{-\Delta\Delta Ct}$ method. The primer sequences used in this study were obtained from PrimerBank (Wang et al., 2012) and produced by IDT (Integrated DNA Technologies) as follows: *Gapdh* (forward primer 5′-AGGTCGGTGTGAACGGATTTG-3′, reverse primer 5′-TGTAGAC-CATGTAGTTGAGGTCA-3′), *Tcf7l2* (forward primer 5′-GCACACA-TCGTTCAGAGCC-3′, reverse primer 5′-GGGTGTAGAAGTGCG-GACA-3′), *Ttll3v2* (forward primer 5′-ATGGGCCGACTCAGAAACG-3′, reverse primer 5′-CGCAAGAGACACCGGATCA-3′), *Dlk1* (forward primer 5′-CCCAGGTGAGCTTCGAGTG-3′, reverse primer 5′-GGA-GAGGGGTACTCTTGTTGAG-3′) and β-catenin (forward primer

Development (2023) 150, dev201189. doi:10.1242/dev.201189

5′-ATGGAGCCGGACAGAAAAGC-3′, reverse primer 5′-CTTGCCACT-CAGGGAAGGA-3′).

Soft palatal primary cell culture

The soft palate from E13.5 embryos was dissected and digested using Multi Tissue Dissociate Kit 3 (Miltenyi Biotec, 130-110-204) at 37°C in a Thermomixer (600 rpm for 15 min, Thermo Fisher Scientific, 2231000269). After adding the medium to stop the digestion process, filtering through a 70 µm Pre-Separation Filter (Miltenyi Biotec, 130-095-823) and centrifuging at 4°C (300 ***g***, 5 min), cells were seeded on a 24-well plate (0.5×10^5 cell/well) in growth medium (DMEM medium, Thermo Fisher Scientific, 10569010; fetal bovine serum, VWR, 97068-085; 1% penicillin and streptomycin, Thermo Fisher Scientific, 15140122). The 24-well plates were collagen coated (Millipore Sigma, 125-50) before plating the cells. For siRNA treatment, *Tcf7l2* Silencer Select Pre-designed siRNA (Thermo Fisher Scientific, 4390771; s74838), *Ttll3* Silencer Select Pre-designed siRNA (Thermo Fisher Scientific, 4390771; s97693), β-catenin Silencer Select Pre-designed siRNA (Thermo Fisher Scientific, 4390771; s63417) and Silencer Select Negative Control #1 siRNA (Thermo Fisher Scientific, 4390843) were delivered by using Lipofectamine RNAiMAX Transfection Reagent (Thermo Fisher Scientific, 13778-075) according to the manufacturer's instructions. For β-catenin and *Tcf7l2* double siRNA treatment, a half dose of each siRNA was used. The cells were treated with siRNA for 72 h before further analysis.

Palatal shelf slice cultures

Embryonic mouse heads were dissected and embedded on ice in a mixture of preheated gelatin and Accell siRNA delivery culture medium (Horizon, B-005000-500) and sectioned into 300 µm slices using MicroSlicer Zero 1N (Ted Pella, 10111N). These slices were placed on 0.4 µm Millicell cell culture inserts (30 mm, hydrophilic PTFE, Sigma-Aldrich, PICM03050) which were inserted into 6-well culture plates (VWR, 10062-892). Micro-injection of control siRNA (Accell Control siRNA – Green; Horizon; K-005000-G1-02 or Accell Control siRNA – Red; Horizon; K-005000-R1-02), Accell Mouse *Ttll3* siRNA, SMARTPool (20 nmol; Horizon; E-063939-00-0020) or Accell Mouse *Dlk1* siRNA, SMARTPool (20 nmol; Horizon; E-043253-00-0020) was performed at a concentration of 100 µM. Cultures were maintained at 37°C in a 5% CO_2 incubator for 3 days and the culture medium was changed every day.

UCSC/JASPAR binding prediction and CUT&RUN assay

The UCSC/JASPAR bioinformatics database was used to search the promoter regions of individual genes in order to identify the binding profiles of transcription factors related to canonical Wnt signaling. The predicted Tcf7l2-binding sites to the promoter region of *Ttll3* gene were identified at chr6:113388069-113388082. The following primers were used for the CUT&RUN assay: forward, TTGAACATCATGTGGCCCAGT; reverse, CACTGTAAACCAGGGACTGCT. The soft palatal tissue from E13.5 embryos was collected and fixed according to the manufacturer's instructions based on CUT&RUN assay kit (Cell Signaling Technology, 86652). 10 µl of IgG isotype control (Cell Signaling Technology, 3900) or Tcf7l2 (Thermo Fisher Scientific, MA5-14935) were used for each reaction. Embryos from two litters were used for each replicate.

CellChat and SCENIC analysis

Previously generated E13.5 soft palatal tissue single cell analysis data (Han et al., 2021) were processed using Seurat R package. RunPCA and RunUMAP visualization were used for cluster visualization. The data are available in GEO under accession number GSE155928. This dataset was processed with R package SCENIC to identify gene regulatory networks (Aibar et al., 2017). GENIE3 was used to identify the individual transcription factors that were later scored by AUCell. R package CellChat (Jin et al., 2021) was used to recognize the predicted ligand-receptor interactions between individual cell populations in the soft palate. The CellChat workflow was used with standard parameters (pre-processing functions: identifyOverExpressedGenes, identifyOverExpressedInteractions and projectData, core functions: computeCommunProb, computeCommunProbPathway and aggregateNet). netVisual_bubble and netAnalysis_signalingRole_heatmap were used to visualize the predicted results.

Imaging

Immunofluorescence images were captured using a Leica DMI3000 B research microscope. Bright-field images were captured using a Keyence BZ-X710 system at the Center for Craniofacial Molecular Biology, University of Southern California.

Statistical analysis

GraphPad Prism Software (Prism 9) was used for statistical analysis. We used n=3 for all experiments unless otherwise stated. Each data point in the bar graphs represents one biological replicate. For each qPCR experiment, at least three technical replicates were analyzed. For histological staining, immunofluorescence and RNAScope, we used samples from at least three individual mice, or embryos, and representative images are shown. All bar graphs display mean±s.e.m. Statistical comparisons were carried out using an unpaired *t*-test with two-tailed calculations. One-way ANOVA was used for analyzing data for comparison of four independent groups. P<0.05 was treated as statistically significant for all analyses.

Acknowledgements

We are grateful to Bridget Samuels for critical reading of this manuscript, and to Kimi Nakaki and Giselle Mejia for the schematic illustrations. We acknowledge USC Libraries Bioinformatics Service for supporting with analysis of the sequencing data. The bioinformatics software and computing resources were funded by the USC Office of Research and the Norris Medical Library.

Competing interests

The authors declare no competing or financial interests.

Author contributions

Conceptualization: E.J., Y.C.; Methodology: E.J., J.F., T.G., X.H., A.G., A.A.-V., M.S.R., H.Z., T.-V.H., S.P., J.A., Y.C.; Software: T.-V.H.; Validation: E.J., J.F., T.G., A.G., A.A.-V., T.-V.H., S.P., J.A., Y.C.; Formal analysis: E.J., J.F., M.R., H.Z., Y.C.; Investigation: T.G., A.G., Y.C.; Resources: E.J., J.F., T.G., X.H., A.G., A.A.-V., T.-V.H., S.P., J.A., Y.C.; Data curation: E.J., J.F., T.G., X.H., A.G., A.A.-V., M.R., H.Z., T.-V.H., S.P., Y.C.; Writing - original draft: E.J., Y.C.; Writing - review & editing: E.J., Y.C.; Visualization: E.J., J.F., T.G., X.H., A.G., A.A.-V., M.R., H.Z., T.-V.H., J.A., Y.C.; Supervision: Y.C.; Project administration: E.J., J.F., T.G., X.H., A.G., A.A.-V., T.-V.H., Y.C.; Funding acquisition: Y.C.

Funding

This work was supported by the National Institute of Dental and Craniofacial Research, National Institutes of Health (R01 DE012711 and U01 DE028729 to Y.C.). Deposited in PMC for release after 12 months.

Data availability

The data for the RNA sequencing used in this study have been deposited in GEO (Edgar et al., 2002) and are accessible through GEO series accession number GSE208619. Previously generated E13.5 soft palatal tissue single cell analysis data (Han et al., 2021) and are available in GEO under accession number GSE155928.

Peer review history

The peer review history is available online at https://journals.biologists.com/dev/lookup/doi/10.1242/dev.201189.reviewer-comments.pdf

References

Aibar, S., Gonzalez-Blas, C. B., Moerman, T., Van, A. H. T., Imrichova, H., Hulselmans, G., Rambow, F., Marine, J. C., Geurts, P., Aerts, J. et al. (2017). SCENIC: single-cell regulatory network inference and clustering. *Nat. Methods* **14**, 1083-1086. doi:10.1038/nmeth.4463

Boletta, A., Qian, F., Onuchic, L. F., Bhunia, A. K., Phakdeekitcharoen, B., Hanaoka, K., Guggino, W., Monaco, L. and Germino, G. G. (2000). Polycystin-1, the gene product of PKD1, induces resistance to apoptosis and spontaneous tubulogenesis in MDCK cells. *Mol. Cell* **6**, 1267-1273. doi:10.1016/S1097-2765(00)00123-4

Brault, V., Moore, R., Kutsch, S., Ishibashi, M., Rowitch, D. H., Mcmahon, A. P., Sommer, L., Boussadia, O. and Kemler, R. (2001). Inactivation of the β-catenin gene by Wnt1-Cre-mediated deletion results in dramatic brain malformation and failure of craniofacial development. *Development* **128**, 1253-1264. doi:10.1242/dev.128.8.1253

Brugmann, S. A., Allen, N. C., James, A. W., Mekonnen, Z., Madan, E. and Helms, J. A. (2010a). A primary cilia-dependent etiology for midline facial disorders. *Hum. Mol. Genet.* **19**, 1577-1592. doi:10.1093/hmg/ddq030

Brugmann, S. A., Cordero, D. R. and Helms, J. A. (2010b). Craniofacial ciliopathies: a new classification for craniofacial disorders. *Am. J. Med. Genet. A* **152A**, 2995-3006. doi:10.1002/ajmg.a.33727

Cadigan, K. M. and Waterman, M. L. (2012). TCF/LEFs and Wnt signaling in the nucleus. *Cold Spring Harbor Perspect. Biol.* **4**, a007906. doi:10.1101/cshperspect.a007906

Cantagrel, V., Silhavy, J. L., Bielas, S. L., Swistun, D., Marsh, S. E., Bertrand, J. Y., Audollent, S., Attie-Bitach, T., Holden, K. R., Dobyns, W. B. et al. (2008). Mutations in the cilia gene ARL13B lead to the classical form of Joubert syndrome. *Am. J. Hum. Genet.* **83**, 170-179. doi:10.1016/j.ajhg.2008.06.023

Caron, A., Xu, X. L. and Lin, X. Y. (2012). Wnt/β-catenin signaling directly regulates Foxj1 expression and ciliogenesis in zebrafish Kupffer's vesicle. *Development* **139**, 514-524. doi:10.1242/dev.071746

Caspary, T., Larkins, C. E. and Anderson, K. V. (2007). The graded response to sonic hedgehog depends on cilia architecture. *Dev. Cell* **12**, 767-778. doi:10.1016/j.devcel.2007.03.004

Chen, J. Q., Lan, Y., Baek, J. A., Gao, Y. and Jiang, R. L. (2009). Wnt/β-catenin signaling plays an essential role in activation of odontogenic mesenchyme during early tooth development. *Dev. Biol.* **334**, 174-185. doi:10.1016/j.ydbio.2009.07.015

Contreras, O., Soliman, H., Theret, M., Rossi, F. M. V. and Brandan, E. (2020). TGF-β-driven downregulation of the transcription factor TCF7L2 affects Wnt/β-catenin signaling in PDGFR α(+) fibroblasts. *J. Cell Sci.* **133**, jcs242297. doi:10.1242/jcs.242297

Corbit, K. C., Shyer, A. E., Dowdle, W. E., Gaulden, J., Singla, V. and Reiter, J. F. (2008). Kif3a constrains β-catenin-dependent Wnt signalling through dual ciliary and non-ciliary mechanisms. *Nat. Cell Biol.* **10**, 70-76. doi:10.1038/ncb1670

Dixon, M. J., Marazita, M. L., Beaty, T. H. and Murray, J. C. (2011). Cleft lip and palate: understanding genetic and environmental influences. *Nat. Rev. Genet.* **12**, 167-178. doi:10.1038/nrg2933

Edgar, R., Domrachev, M. and Lash, A. E. (2002). Gene Expression Omnibus: NCBI gene expression and hybridization array data repository. *Nucleic Acids Res.* **30**, 207-210. doi:10.1093/nar/30.1.207

Feng, J., Han, X., Yuan, Y., Cho, C. K., Janeckova, E., Guo, T., Pareek, S., Rahman, M. S., Zheng, B., Bi, J. et al. (2022). TGF- β signaling and Creb5 cooperatively regulate Fgf18 to control pharyngeal muscle development. *Elife* **11**, e80405. doi:10.7554/eLife.80405

Fu, W. X., Asp, P., Canter, B. and Dynlacht, B. D. (2014). Primary cilia control hedgehog signaling during muscle differentiation and are deregulated in rhabdomyosarcoma. *Proc. Natl. Acad. Sci. USA* **111**, 9151-9156. doi:10.1073/pnas.1323265111

Gadadhar, S., Dadi, H., Bodakuntla, S., Schnitzler, A., Bieche, I., Rusconi, F. and Janke, C. (2017). Tubulin glycylation controls primary cilia length. *J. Cell Biol.* **216**, 2701-2713. doi:10.1083/jcb.201612050

Grimaldi, A., Parada, C. and Chai, Y. (2015). A comprehensive study of soft palate development in mice. *PLoS One* **10**, e0145018. doi:10.1371/journal.pone.0145018

Han, X., Feng, J. F., Guo, T. W., Loh, Y. H. E., Yuan, Y., Ho, T. V., Cho, C. K., Li, J. Y., Jing, J. J., Janeckova, E. et al. (2021). Runx2-Twist1 interaction coordinates cranial neural crest guidance of soft palate myoaenesis. *Elife* **10**, e62387. doi:10.7554/eLife.62387

He, F. L., Xiong, W., Wang, Y., Li, L., Liu, C., Yamagami, T., Taketo, M. M., Zhou, C. J. and Chen, Y. P. (2011). Epithelial Wnt/β-catenin signaling regulates palatal shelf fusion through regulation of Tgf β 3 expression. *Dev. Biol.* **350**, 511-519. doi:10.1016/j.ydbio.2010.12.021

Huelsken, J., Vogel, R., Brinkmann, V., Erdmann, B., Birchmeier, C. and Birchmeier, W. (2000). Requirement for β-catenin in anterior-posterior axis formation in mice. *J. Cell Biol.* **148**, 567-578. doi:10.1083/jcb.148.3.567

Ip, W., Shao, W. J., Chiang, Y. T. A. and Jin, T. R. (2012). The Wnt signaling pathway effector TCF7L2 is upregulated by insulin and represses hepatic gluconeogenesis. *Am. J. Physiol. Endocrinol. Metab.* **303**, E1166-E1176. doi:10.1152/ajpendo.00249.2012

Irigoin, F. and Badano, J. L. (2011). Keeping the balance between proliferation and differentiation: the primary cilium. *Curr. Genomics* **12**, 285-297. doi:10.2174/138920211795860134

Iwata, J., Suzuki, A., Yokota, T., Ho, T. V., Pelikan, R., Urata, M., Sanchez-Lara, P. A. and Chai, Y. (2014). TGF β regulates epithelial-mesenchymal interactions through WNT signaling activity to control muscle development in the soft palate. *Development* **141**, 909-917. doi:10.1242/dev.103093

Janeckova, E., Feng, J., Li, J., Rodriguez, G. and Chai, Y. (2019). Dynamic activation of Wnt, Fgf, and Hh signaling during soft palate development. *PLoS One* **14**, 1-16. doi:10.1371/journal.pone.0223879

Jin, S. Q., Guerrero-Juarez, C. F., Zhang, L. H., Chang, I., Ramos, R., Kuan, C. H., Myung, P., Plikus, M. V. and Nie, Q. (2021). Inference and analysis of cell-cell communication using CellChat. *Nat. Commun.* **12**, 1088. doi:10.1038/s41467-021-21246-9

Kardon, G., Harfe, B. D. and Tabin, C. J. (2003). A Tcf4-positive mesodermal population provides a prepattern for vertebrate limb muscle patterning. *Dev. Cell* **5**, 937-944. doi:10.1016/S1534-5807(03)00360-5

Kasahara, K. and Inagaki, M. (2021). Primary ciliary signaling: links with the cell cycle. *Trends Cell Biol.* **31**, 954-964. doi:10.1016/j.tcb.2021.07.009

Kim, K., Cho, J., Hilzinger, T. S., Nuuns, H., Liu, A., Ryba, B. E. and Goentoro, L. (2017). Two-element transcriptional regulation in the canonical Wnt pathway. *Curr. Biol.* **27**, 2357-2364.e5. doi:10.1016/j.cub.2017.06.037

Kyun, M. L., Kim, S. O., Lee, H. G., Hwang, J. A., Hwang, J., Soung, N. K., Cha-Molstad, H., Lee, S., Kwon, Y. T., Kim, B. Y. et al. (2020). Wnt3a stimulation promotes primary ciliogenesis through β-catenin phosphorylation-induced reorganization of centriolar satellites. *Cell Rep.* **30**, 1447-1462.e5. doi:10.1016/j.celrep.2020.01.019

Li, J., Rodriguez, G., Han, X., Janeckova, E., Kahng, S., Song, B. and Chai, Y. (2019). Regulatory mechanisms of soft palate development and malformations. *J. Dent. Res.* **98**, 959-967. doi:10.1177/0022034519851786

Liu, W. J., Lan, Y., Pauws, E., Meester-Smoor, M. A., Stanier, P., Zwarthoff, E. C. and Jiang, R. L. (2008). The Mn1 transcription factor acts upstream of Tbx22 and preferentially regulates posterior palate growth in mice. *Development* **135**, 3959-3968. doi:10.1242/dev.025304

Liu, L., Xu, Z. W., Jiang, Y. Y., Karim, M. R. and Huang, X. (2021). Cell cycle regulation through primary cilium: A long-forgotten story. *Biocell* **45**, 823-833. doi:10.32604/biocell.2021.013864

Marrinan, E. M., Labrie, R. A. and Mulliken, J. B. (1998). Velopharyngeal function in nonsyndromic cleft palate: Relevance of surgical technique, age at repair, and cleft type. *Cleft Palate Craniofac. J.* **35**, 95-100. doi:10.1597/1545-1569_1998_035_0095_vfincp_2.3.co_2

Monroy, P. L. C., Grefte, S., Kuijpers-Jagtman, A. M., Wagener, F. and Von Den Hoff, J. W. (2012). Strategies to improve regeneration of the soft palate muscles after cleft palate repair. *Tissue Eng. B Rev.* **18**, 468-477. doi:10.1089/ten.teb.2012.0049

Monroy, P. L. C., Grefte, S., Kuijpers-Jagtman, A. M., Helmich, M. P. A. C., Wagener, F. A. D. T. G. and Von Den Hoff, J. W. (2015). Fibrosis impairs the formation of new myofibers in the soft palate after injury. *Wound Repair. Regen.* **23**, 866-873. doi:10.1111/wrr.12345

Noden, D. M. and Francis-West, P. (2006). The differentiation and morphogenesis of craniofacial muscles. *Dev. Dyn.* **235**, 1194-1218. doi:10.1002/dvdy.20697

Ocbina, P. J. R., Tuson, M. and Anderson, K. V. (2009). Primary cilia are not required for normal canonical Wnt signaling in the mouse embryo. *PLoS One* **4**, e6839. doi:10.1371/journal.pone.0006839.

Ohsugi, T., Yamaguchi, K., Zhu, C., Ikenoue, T. and Furukawa, Y. (2017). Decreased expression of interferon-induced protein 2 (IFIT2) by Wnt/β-catenin signaling confers anti-apoptotic properties to colorectal cancer cells. *Oncotarget* **8**, 100176-100186. doi:10.18632/oncotarget.22122

Poretti, A., Vitiello, G., Hennekam, R. C. M., Arrigoni, F., Bertini, E., Borgatti, R., Brancati, F., D'arrigo, S., Faravelli, F., Giordano, L. et al. (2012). Delineation and diagnostic criteria of oral-facial-digital syndrome type VI. *Orphanet J. Rare Dis.* **7**, 4. doi:10.1186/1750-1172-7-4

Reynolds, K., Kumari, P., Rincon, L. S., Gu, R., Ji, Y., Kumar, S. and Zhou, C. J. J. (2019). Wnt signaling in orofacial clefts: crosstalk, pathogenesis and models. *Dis. Model. Mech.* **12**, dmm037051. doi:10.1242/dmm.037051

Sambasivan, R., Kuratani, S. and Tajbakhsh, S. (2011). An eye on the head: the development and evolution of craniofacial muscles. *Development* **138**, 2401-2415. doi:10.1242/dev.040972

Schock, E. N. and Brugmann, S. A. (2017). Discovery, diagnosis, and etiology of craniofacial ciliopathies. *Cold Spring Harbor Perspect. Biol.* **9**, a028258. doi:10.1101/cshperspect.a028258

Shin, S., Suh, Y., Zerby, H. N. and Lee, K. (2014). Membrane-bound delta-like 1 homolog (Dlk1) promotes while soluble Dlk1 inhibits myogenesis in C2C12 cells. *FEBS Lett.* **588**, 1100-1108. doi:10.1016/j.febslet.2014.02.027

Simons, M., Gloy, J., Ganner, A., Bullerkotte, A., Bashkurov, M., Kronig, C., Schermer, B., Benzing, T., Cabello, O. A., Jenny, A. et al. (2005). Inversin, the gene product mutated in nephronophthisis type II, functions as a molecular switch between Wnt signaling pathways. *Nat. Genet.* **37**, 537-543. doi:10.1038/ng1552

Skene, P. J. and Honikoff, S. (2017). An efficient targeted nuclease strategy for high-resolution mapping of DNA binding sites. *Elife* **6**, e21856. doi:10.7554/eLife.21856

Strand, D. W., Franco, O. E., Basanta, D., Anderson, A. R. A. and Hayward, S. W. (2010). Perspectives on tissue interactions in development and disease. *Curr. Mol. Med.* **10**, 95-112. doi:10.2174/156652410791065363

Sugii, H., Grimaldi, A., Li, J. Y., Parada, C., Thach, V. H., Feng, J. F., Jing, J. J., Yuan, Y., Guo, Y. X., Maeda, H. et al. (2017). The Dlx5-FGF10 signaling cascade controls cranial neural crest and myoblast interaction during oropharyngeal patterning and development. *Development* **144**, 4037-4045. doi:10.1242/dev.155176

Suzuki, A., Minamide, R. and Iwata, J. (2018). WNT/β-catenin signaling plays a crucial role in myoblast fusion through regulation of nephrin expression during development. *Development* **145**, dev168351. doi:10.1242/dev.168351

Tian, H., Feng, J. F., Li, J. Y., Ho, T. V., Yuan, Y., Liu, Y., Brindopke, F., Figueiredo, J. C., Magee, W., Sanchez-Lara, P. A. et al. (2017). Intraflagellar

transport 88 (IFT88) is crucial for craniofacial development in mice and is a candidate gene for human cleft lip and palate. *Hum. Mol. Genet.* **26**, 860-872. doi:10.1093/hmg/ddx002

Von Den Hoff, J. W., Carvajal Monroy, P. L., Ongkosuwito, E. M., Van Kuppevelt, T. H. and Daamen, W. F. (2018). Muscle fibrosis in the soft palate: Delivery of cells, growth factors and anti-fibrotics. *Adv. Drug. Deliv. Rev.* **146**, 60-76. doi:10.1016/j.addr.2018.08.002

Waddell, J. N., Zhang, P. J., Wen, Y. F., Gupta, S. K., Yevtodiyenko, A., Schmidt, J. V., Bidwell, C. A., Kumar, A. and Kuang, S. H. (2010). Dlk1 is necessary for proper skeletal muscle development and regeneration. *PLoS One* **5**, e15055. doi:10.1371/journal.pone.0015055

Wang, J. and Barr, M. M. (2018). Cell-cell communication via ciliary extracellular vesicles: clues from model systems. *Essays Biochem.* **62**, 205-213. doi:10.1042/EBC20170085

Wang, X. W., Spandidos, A., Wang, H. J. and Seed, B. (2012). PrimerBank: a PCR primer database for quantitative gene expression analysis, 2012 update. *Nucleic Acids Res.* **40**, D1144-D1149. doi:10.1093/nar/gkr1013

Wehby, G. L. and Cassell, C. H. (2010). The impact of orofacial clefts on quality of life and healthcare use and costs. *Oral Dis.* **16**, 3-10. doi:10.1111/j.1601-0825.2009.01588.x

Wheway, G., Nazlamova, L. and Hancock, J. T. (2018). Signaling through the primary cilium. *Front. Cell Dev. Biol.* **6**, 1-13. doi:10.3389/fcell.2018.00008

Zhong, Z., Zhao, H., Mayo, J. and Chai, Y. (2015). Different requirements for Wnt signaling in tongue myogenic subpopulations. *J. Dent. Res.* **94**, 421-429. doi:10.1177/0022034514566030

Ziermann, J. M., Diogo, R. and Noden, D. M. (2018). Neural crest and the patterning of vertebrate craniofacial muscles. *Genesis* **56**, e23097. doi:10.1002/dvg.23097